Interstellar Medium

Introduction

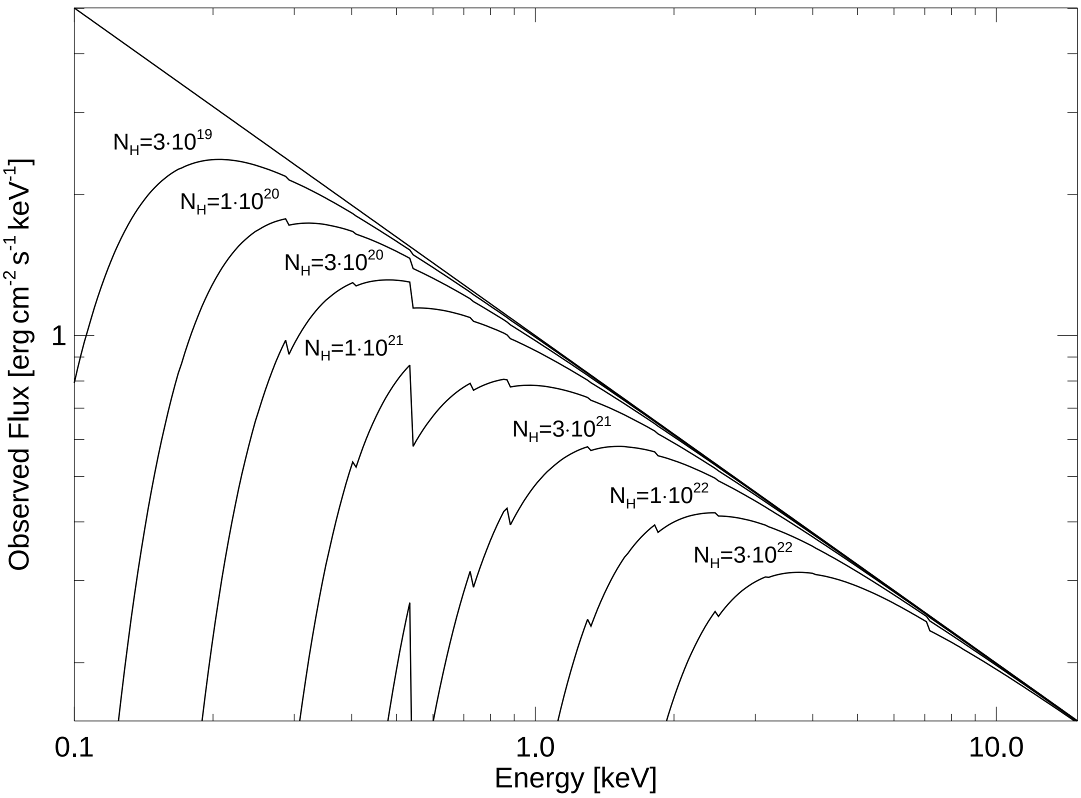

Effect of intermediate medium of Hydrogen column density N_H on observed X-ray spectrum.

$$I_\mathrm{obs}(E) = \mathrm{e}^{-\sigma_\mathrm{ISM}(E)\,N_\mathrm{H}}\, I_\mathrm{source}(E)$$

where

N_H: Hydrogen column density (atoms cm^{-2})

I_source: emitted X-ray spectrum

I_obs: observed X-ray spectrum

IAAT

Previous Formulations

Five important historical papers:

Brown & Gould (1970): First real computations using o.k. cross sections.

Fireman (1974): Include effect of iron, first attempt to formulate influence of dust.

Ride & Walker (1977): Dust and phases of ISM. Largely ignored.

Morrison & McCammon (1983): The *de facto* standard (XSPEC: `model wabs` ...). No dust, fixed abundances.

Bałucińska-Church & McCammon (1992): Better cross sections, based on Henke et al. (1982), newer (and variable) abundances. No dust or molecules. Unfortunately often ignored (XSPEC: `model phabs` ...).

$\Longrightarrow$ Critical reevaluation of computation of σ_{ISM} necessary.

IAAT

Computation

σ_{ISM} = sum over contributions of astrophysically relevant elements:

$$\sigma_{\text{ISM}} = \sigma_{\text{gas}} + \sigma_{\text{grains}} + \sigma_{\text{molecules}}$$

Gas and Molecules:

$$\sigma_{\text{gas, molecules}} = \sum_{Z,I} A_Z \cdot a_{Z,I} \cdot (1 - \beta_{Z,I}) \cdot \sigma_{\text{bf}}(Z, I)$$

where

- Z nuclear charge
- A_Z abundance in number wrt H
- $a_{Z,I}$ ionization fraction
- $1 - \beta_{Z,I}$ depletion factor
- $\sigma_{\text{bf}}(Z, I)$ photoionization cross section

Dust:

$$\sigma_{\text{grains}} = \sum_{Z,I} A_Z \cdot \beta_{Z,I} f_{Z,I} \cdot \sigma_{\text{bf}}(Z, I)$$

where

- $f_{Z,I}$ self blanketing factor

Photoionization cross sections

In X-rays: photon energy $\gg$ binding energy of outer shell electrons $\Longrightarrow$ relativistic QM effects become important.

$\Longrightarrow$ Inner shell processes $\Longrightarrow$ K- and L-shell absorption.

Result of approximate computations: For $E \gg E_{\mathrm{thresh}}$:

$$\sigma_{\mathrm{bf}} \propto E^{-3.5}$$

Experimental measurements are rare.

Compilations of cross sections:

TOPBASE (Seaton et al.): no relativistic effects.

Henke tables (Henke et al., 1982, 1993): combination of experimental and theoretical data.

Verner data (Verner & Yakovlev, 1995): relativistic computations, edge energies adjusted to measured values.

EPDL 97 (Cullen et al., 1997): compilation of measured and theoretical data; not evaluated yet due to export restrictions.

Photoionization cross sections: He

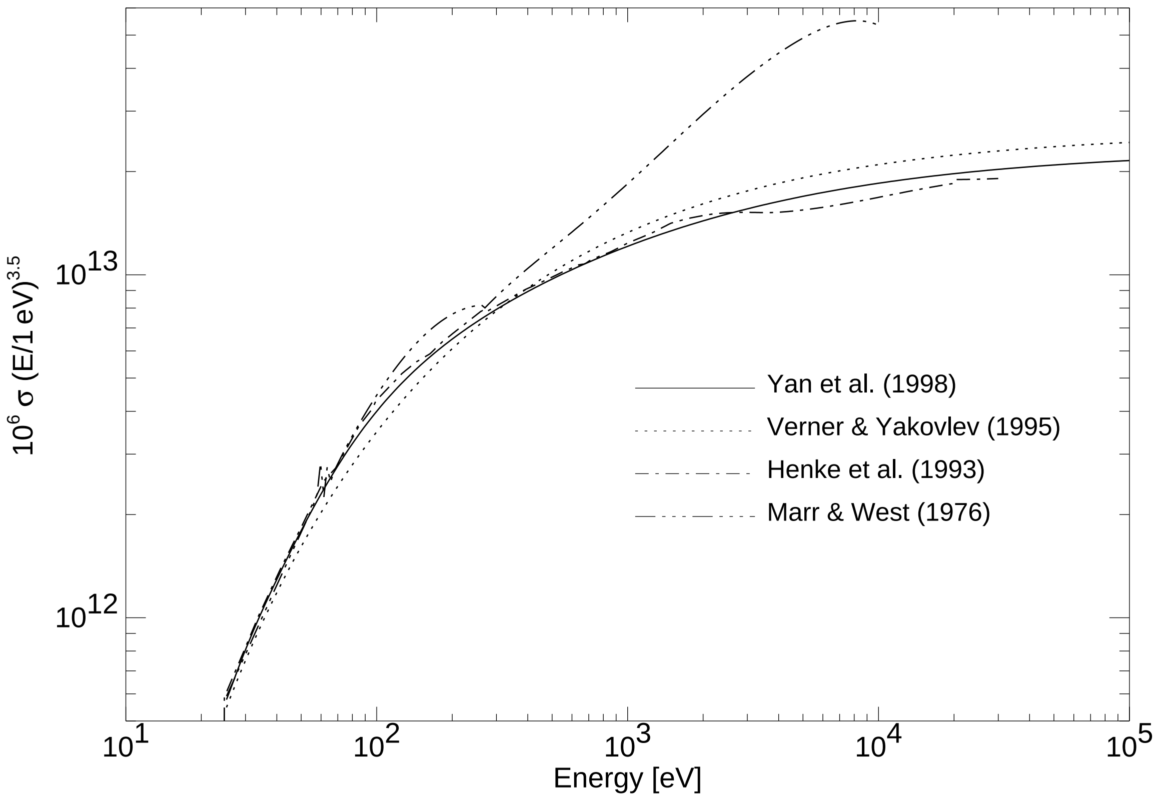

Comparison between four different theories for the He cross section.

For He: Adopt Yan, Sadeghpour & Dalgarno (1998) values.

Photoionization cross sections: Metals

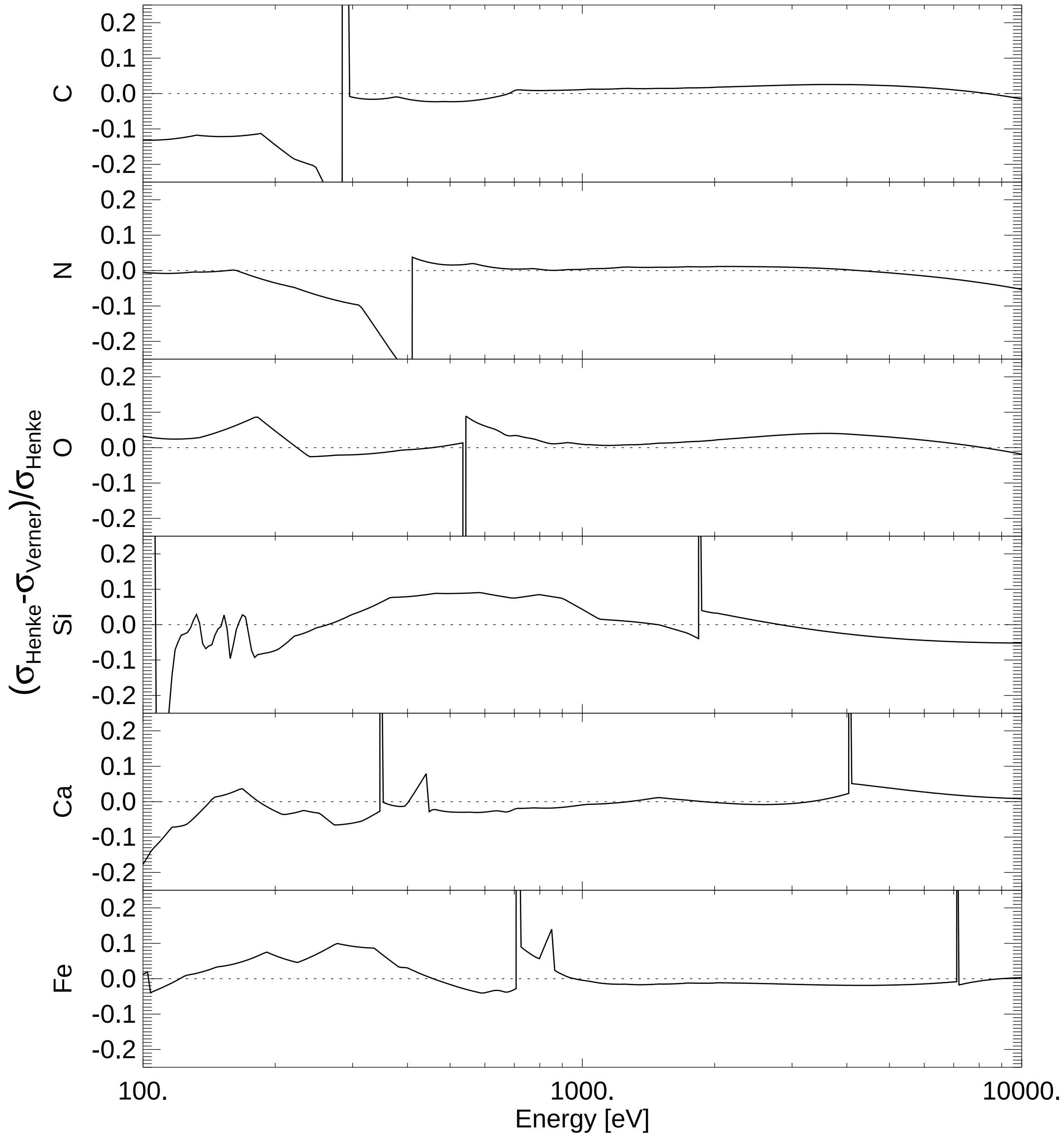

Comparison between the recommended values from Henke et al. (1993) and the theory of Verner & Yakovlev (1995).

Adopt Verner & Yakovlev values.

Solid State Effects

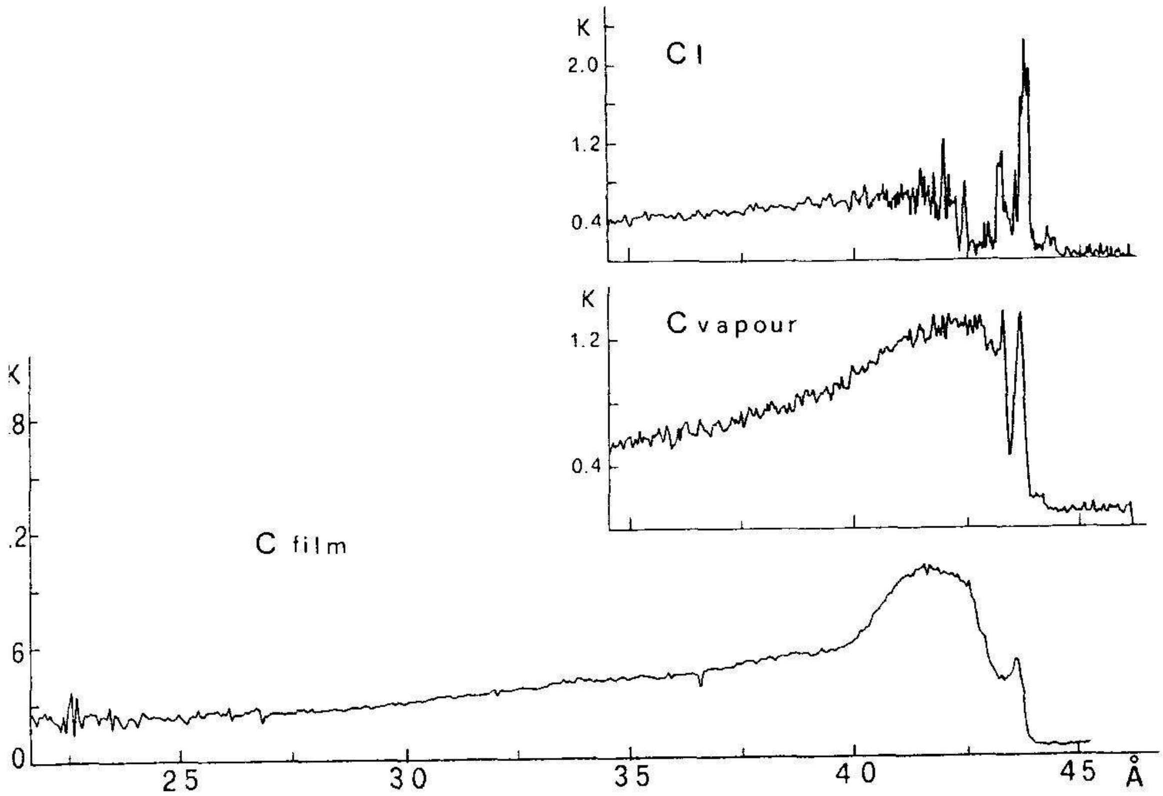

Nicolosi, Jannitti & Tondello (1991)

Strong influence of state of absorbing material on absorptivity $\Longrightarrow$ Edge energies of Henke et al. (1993) are influenced by solid state effects!

Photoionization cross sections: H_2

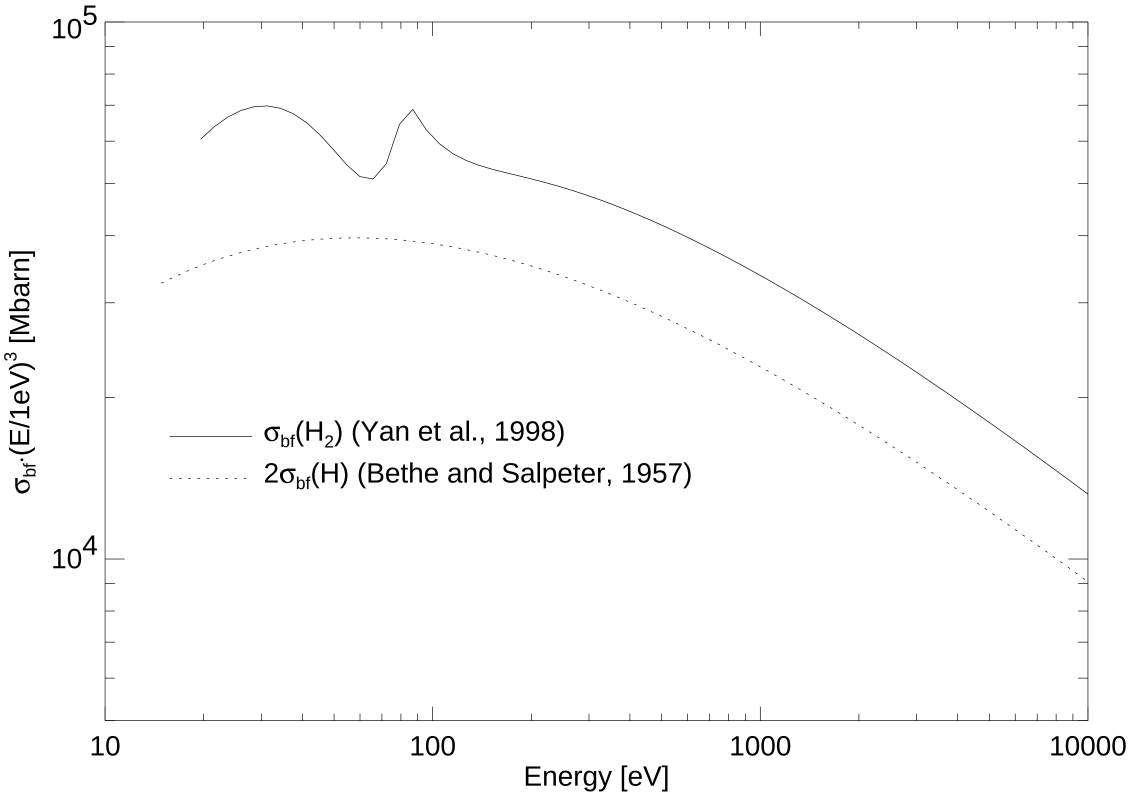

Comparison between classical H cross section and a modern computation of the H_2 cross section.

Molecular effects contribute to absorption cross section: $\sigma_{\text{bf}}(\mathrm{H}_2) \approx 2.85\sigma_{\text{bf}}(\mathrm{H})$.

IAAT

Abundances, I

Basic paradigm during last 50 years of astronomy:
abundances are more or less identical throughout the universe.

⟹ Measurement possible by looking at solar and meteoritic abundances (Anders & Grevesse, 1989).

Recent evidence: ISM abundances are subsolar, dependent on line of sight (Snow & Witt, 1995; Mathis, 1996).

> X-ray astronomical work needs the ability to change abundances relative to the adopted (solar) abundances.

IAAT

Abundances, II

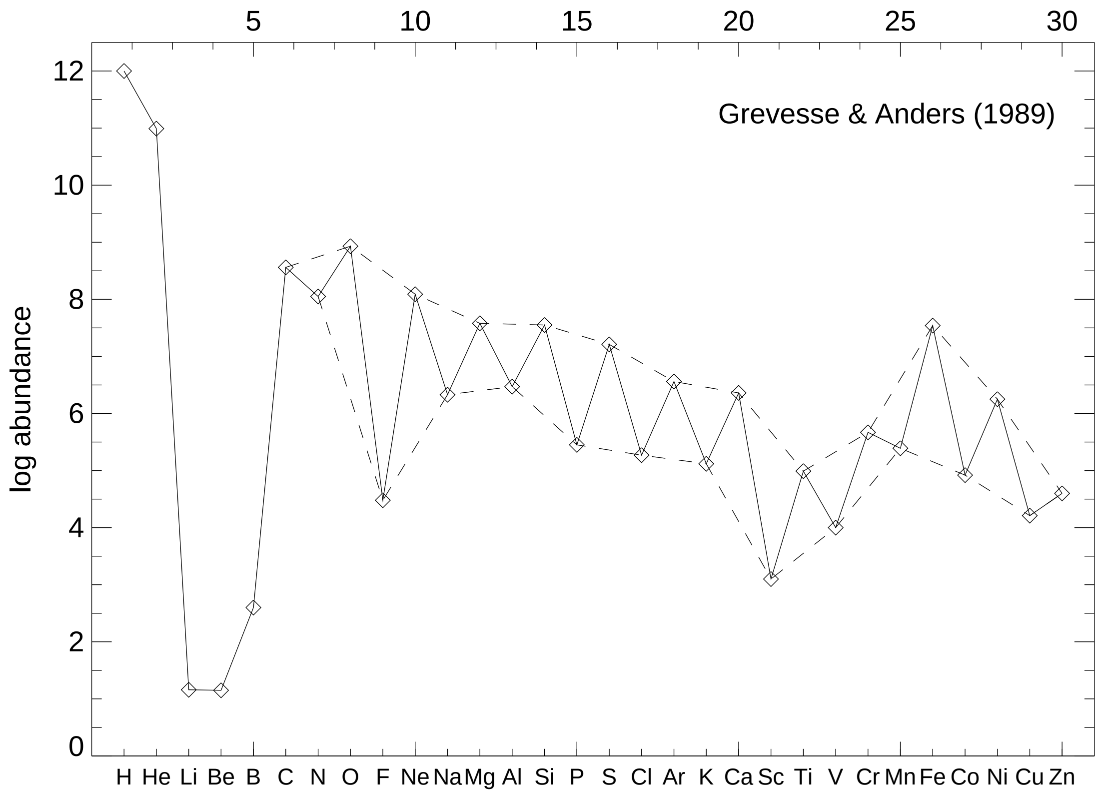

Adopted abundances: solar after Anders & Grevesse (1989) and Grevesse & Anders (1989), for F and Cl use meteoritic values as recommended by Shull (1993).

Odd-Even Z variability due to stability of nuclei with paired protons.

Dust, I

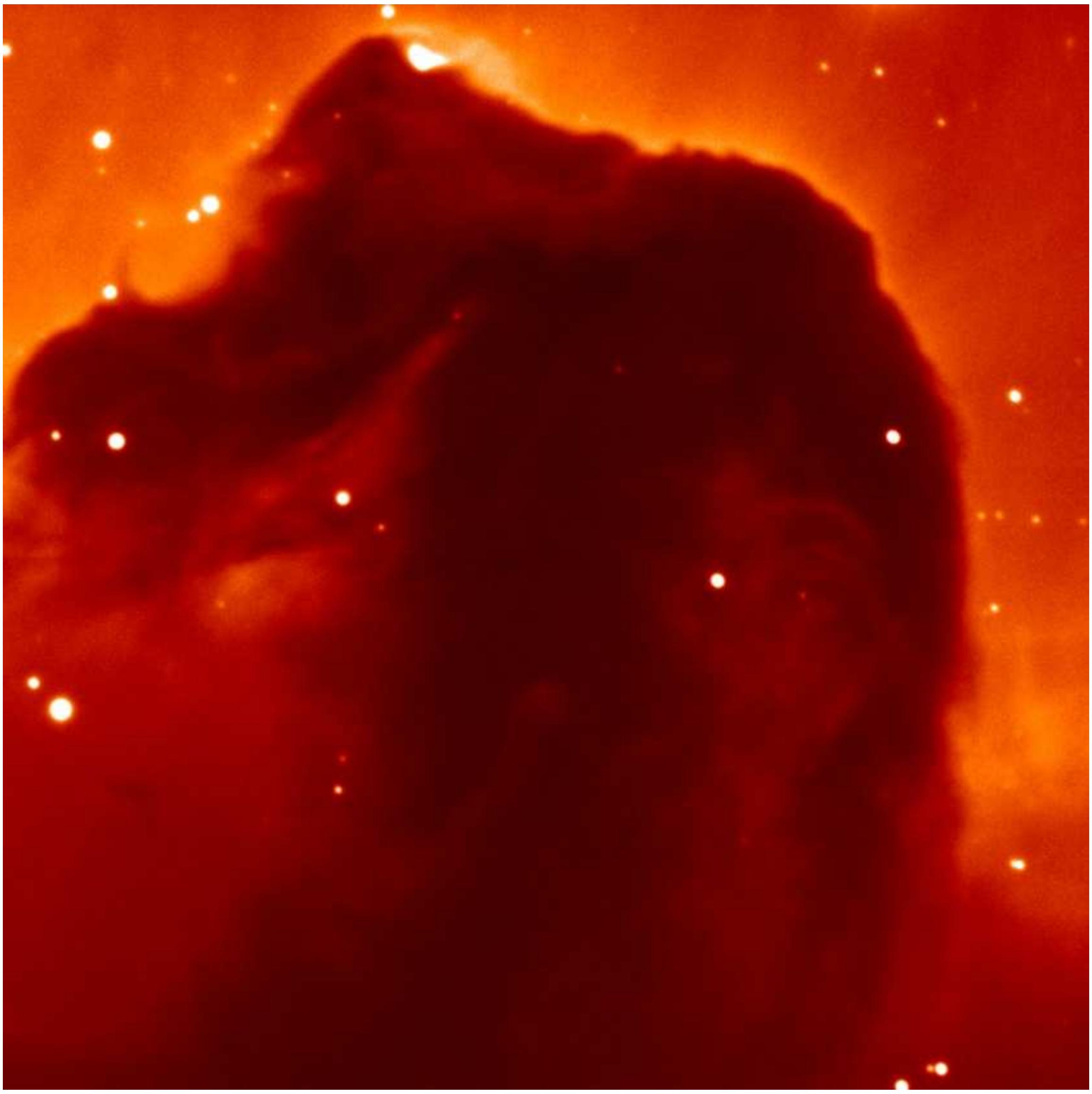

Horsehead nebula (NOT; 2.60 m, Canary Islands).

IAAT

Dust, II

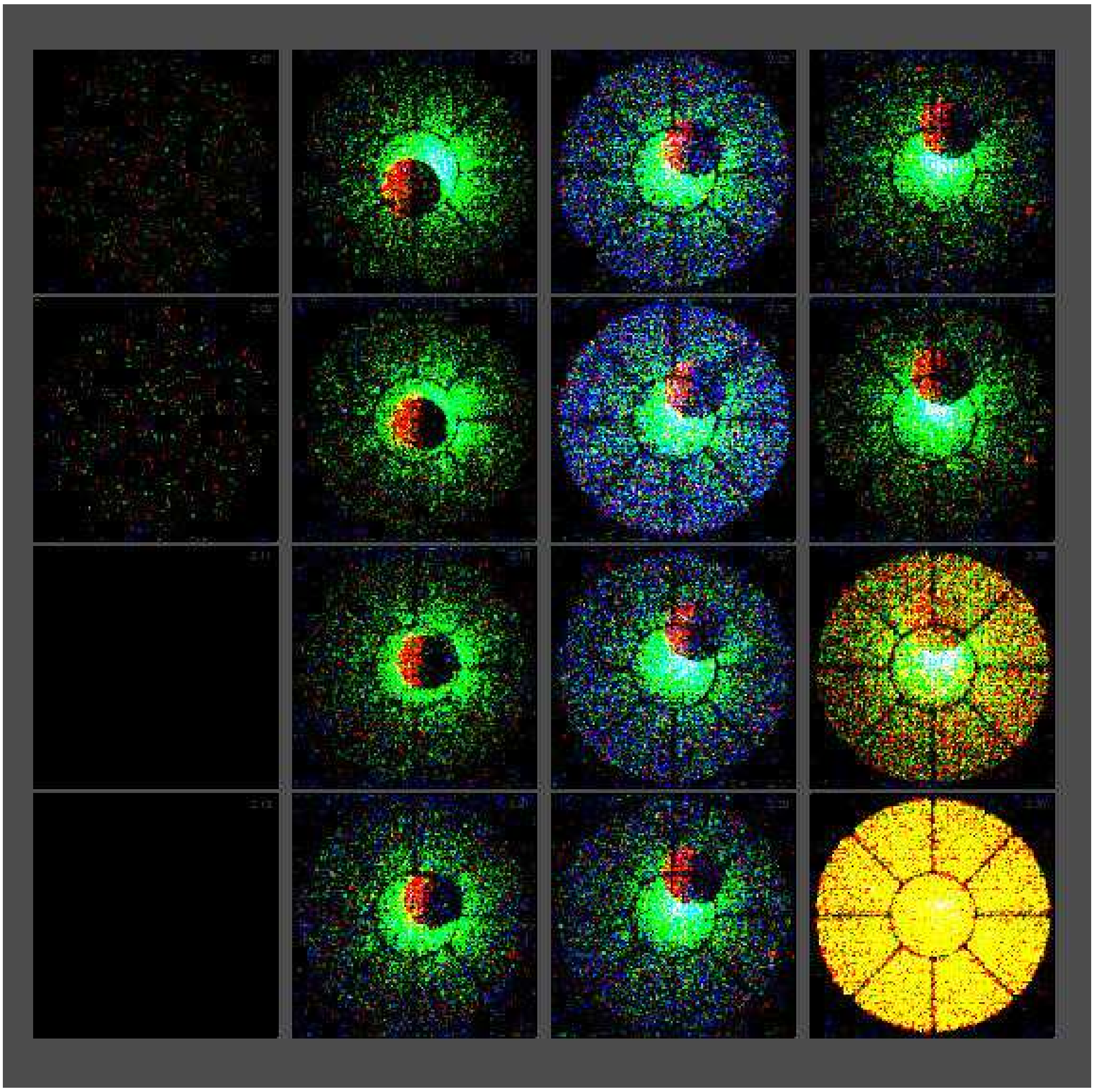

ROSAT: Lunar occultation of Sco X-1 $\Longrightarrow$ X-ray dust scattering halo

Dust, III

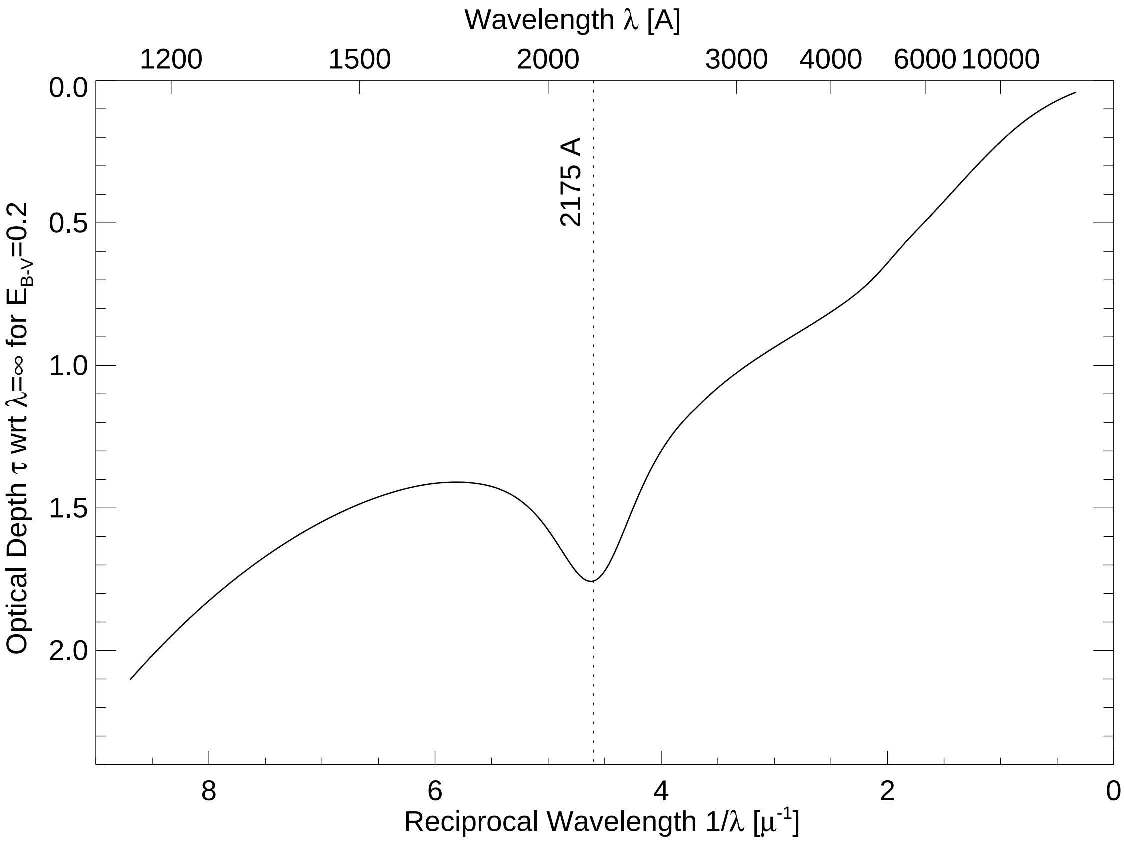

Interstellar reddening curve after Fitzpatrick (1999).

2175 Å bump generally interpreted as evidence for absorption through dust.

Mathis, Rumpl & Nordsieck (1977) (MRN): graphite and silicate grains, power law size distribution, $P(a) \propto a^{-3.5}$, radii ranging from 0.025 μm to 0.25 μm, density $\sim 1\,\mathrm{g\,cm^{-3}}$.

Dust, IV

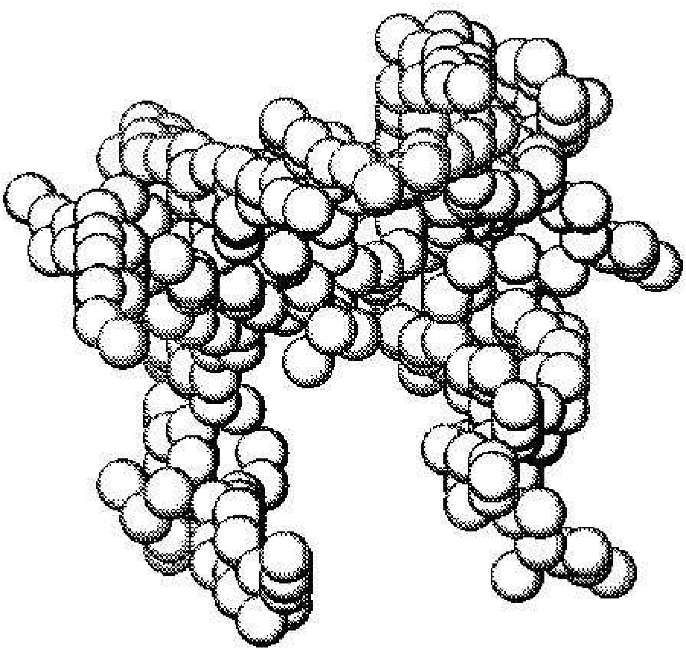

Observational evidence and theoretical motivation favor porous grains composed of silicates, graphite, and oxides (Mathis & Whiffen, 1989; Fogel & Leung, 1998)

$\Longrightarrow$ Density of grains is smaller than $1\,\mathrm{g\,cm^{-3}}$.

Effect of Grains

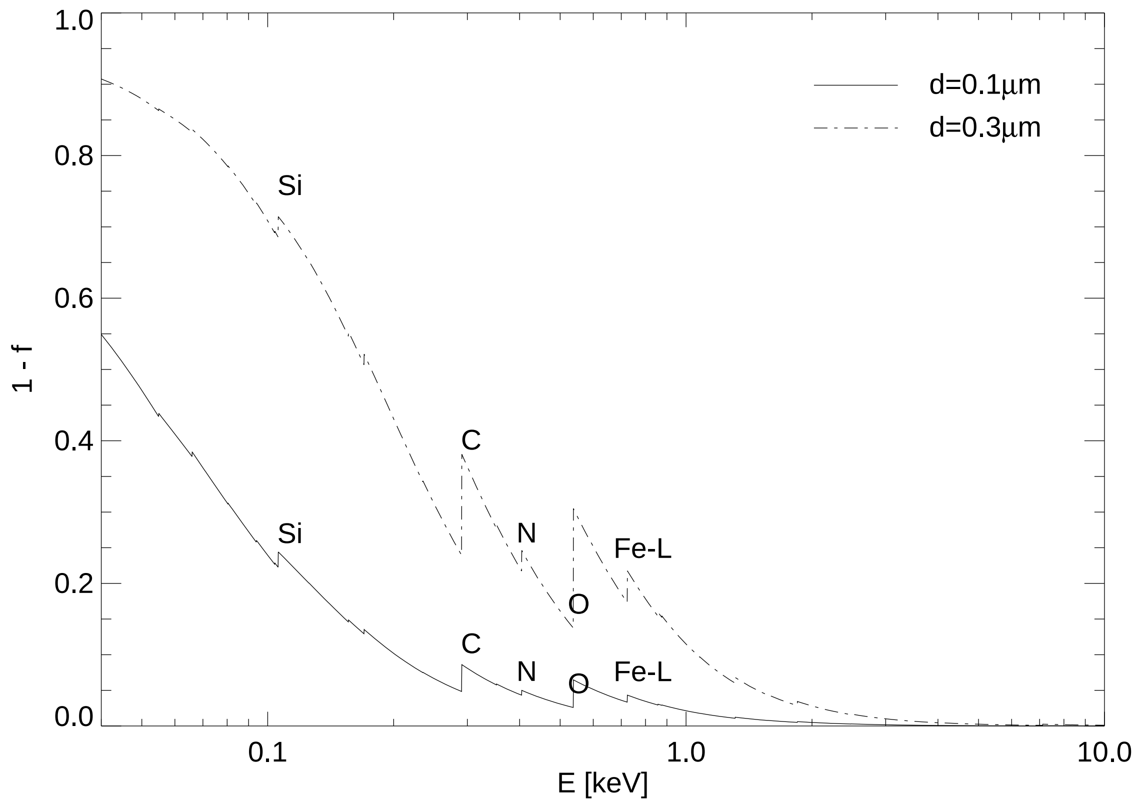

Energy dependent shielding factor for grains of sizes 0.1 μm and 0.3 μm.

X-rays: Metals are "depleted" in grains $\Longrightarrow$ less metals in gas phase.

Outer skin of grains absorbs most X-rays $\Longrightarrow$ do not see inner part of grains $\Longrightarrow$ "shielding"

Computations:

Grains do not have influence above $\sim$3 keV.

Result: Total Absorptivity

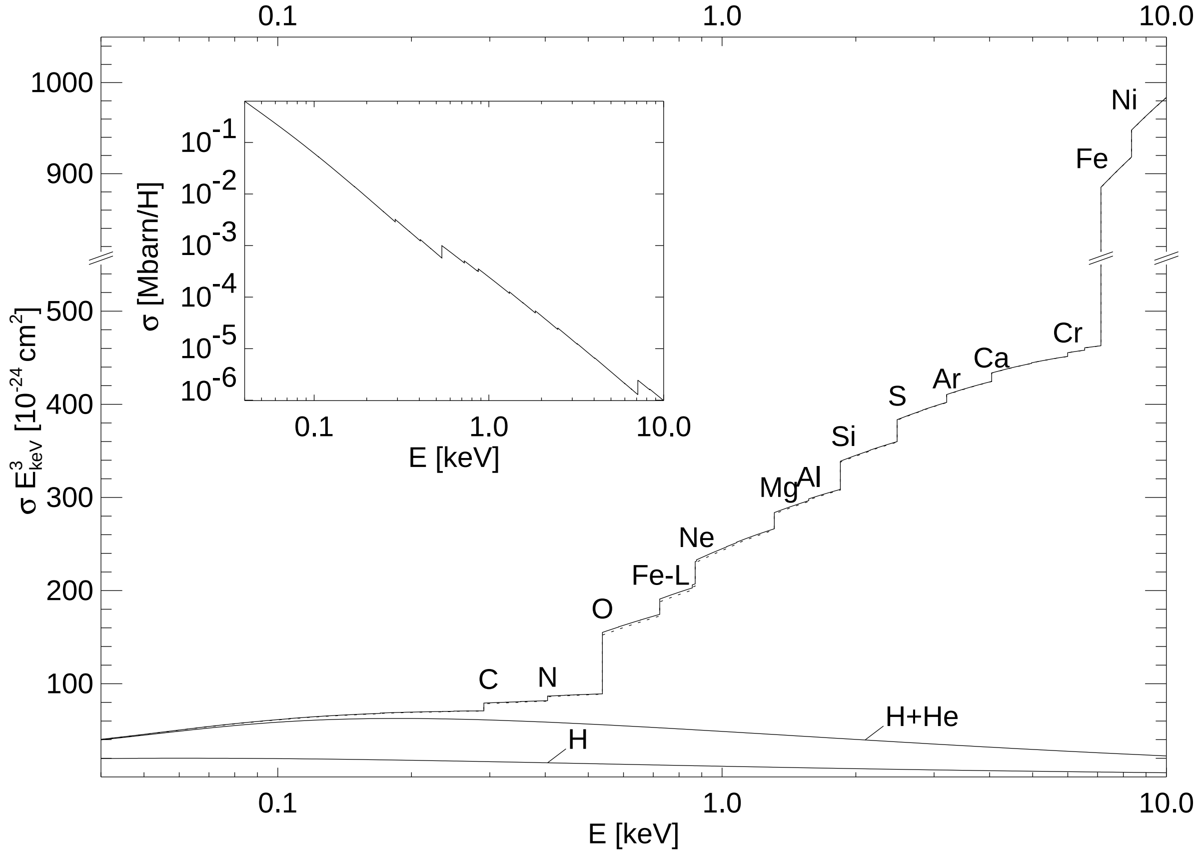

$\sigma_{\text{ISM}} \cdot E^3$ as function of energy for pure gas and for gas with grains with MRN distribution.

Note comparably small influence of grains.

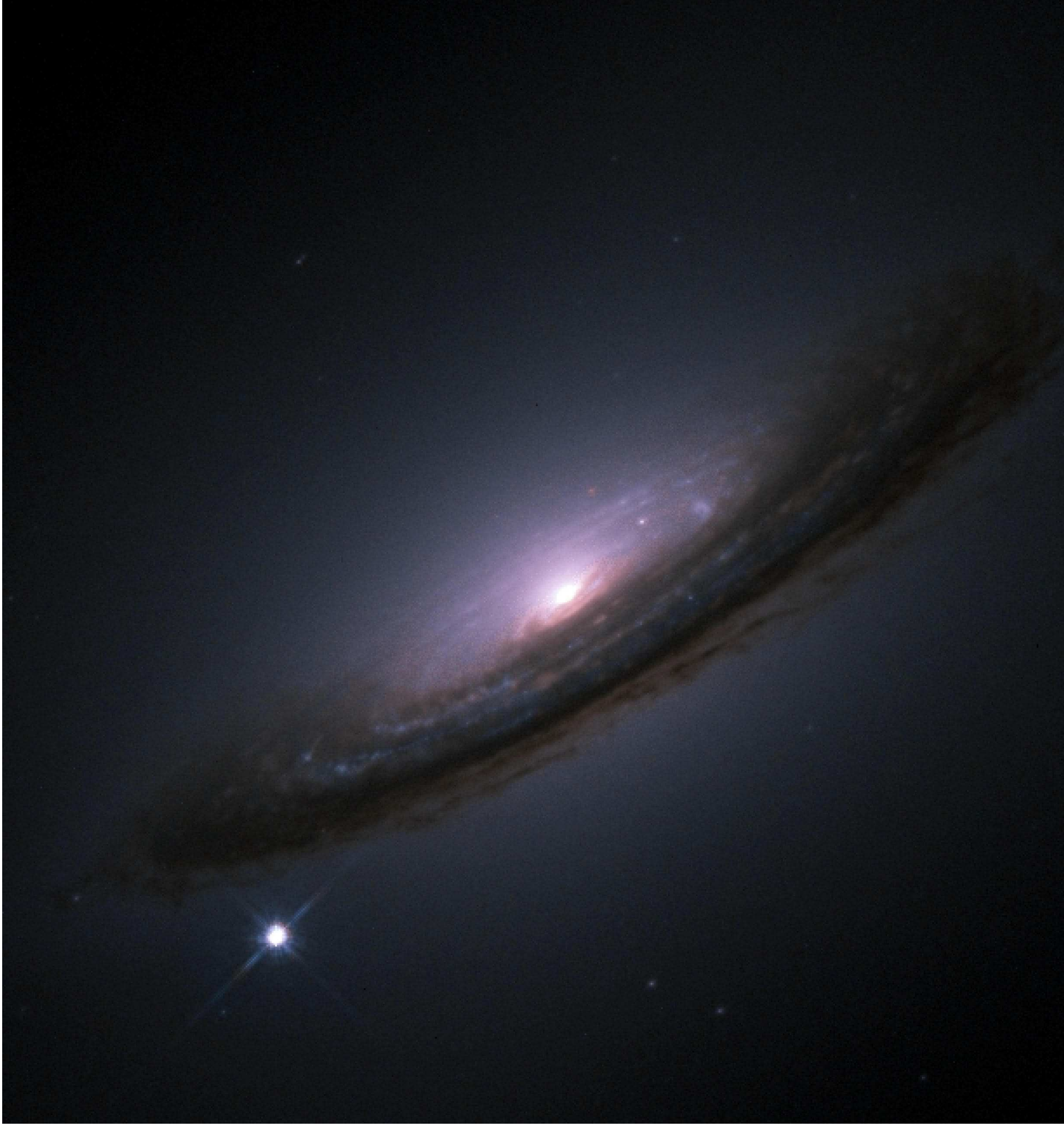

SN1994d (HST WFPC)

Supernovae have luminosities comparable to whole galaxies: $\sim 10^{51}$ erg/s in light, $100\times$ more in neutrinos.

Classifi cation, I

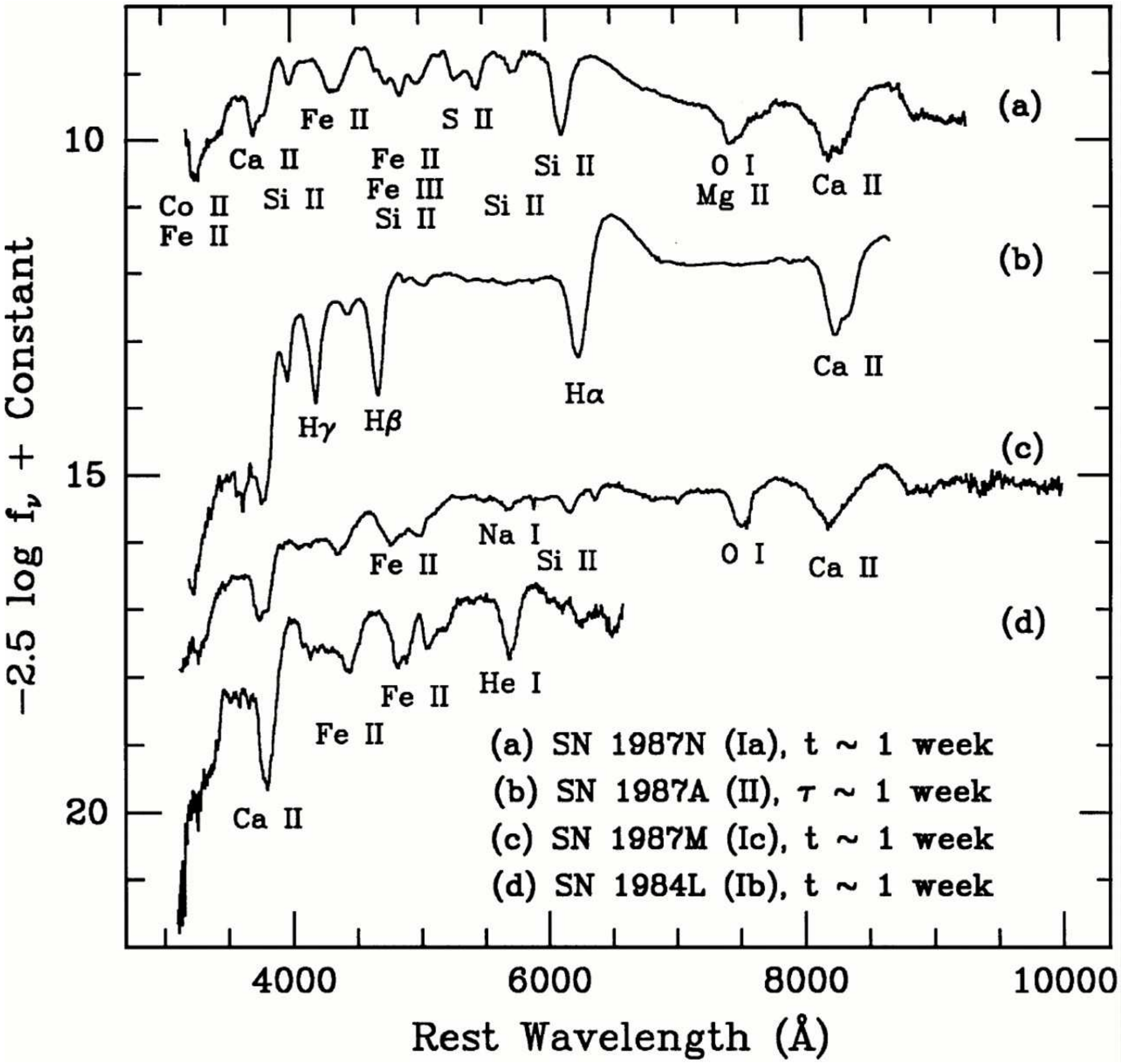

(Filippenko, 1997, Fig. 1); t: time after maximum light; τ: time after core collapse; P Cyg profi les give $v \sim 10000\,\mathrm{km\,s^{-1}}$

Rough classification (Minkowski, 1941):

Type I: no hydrogen in spectra; subtypes Ia, Ib, Ic

Type II: hydrogen present, subtypes II-L, II-P

Note: pre 1985 subtypes Ia, Ib had different defi nition of today $\Longrightarrow$ beware when reading older texts.

Classification, II

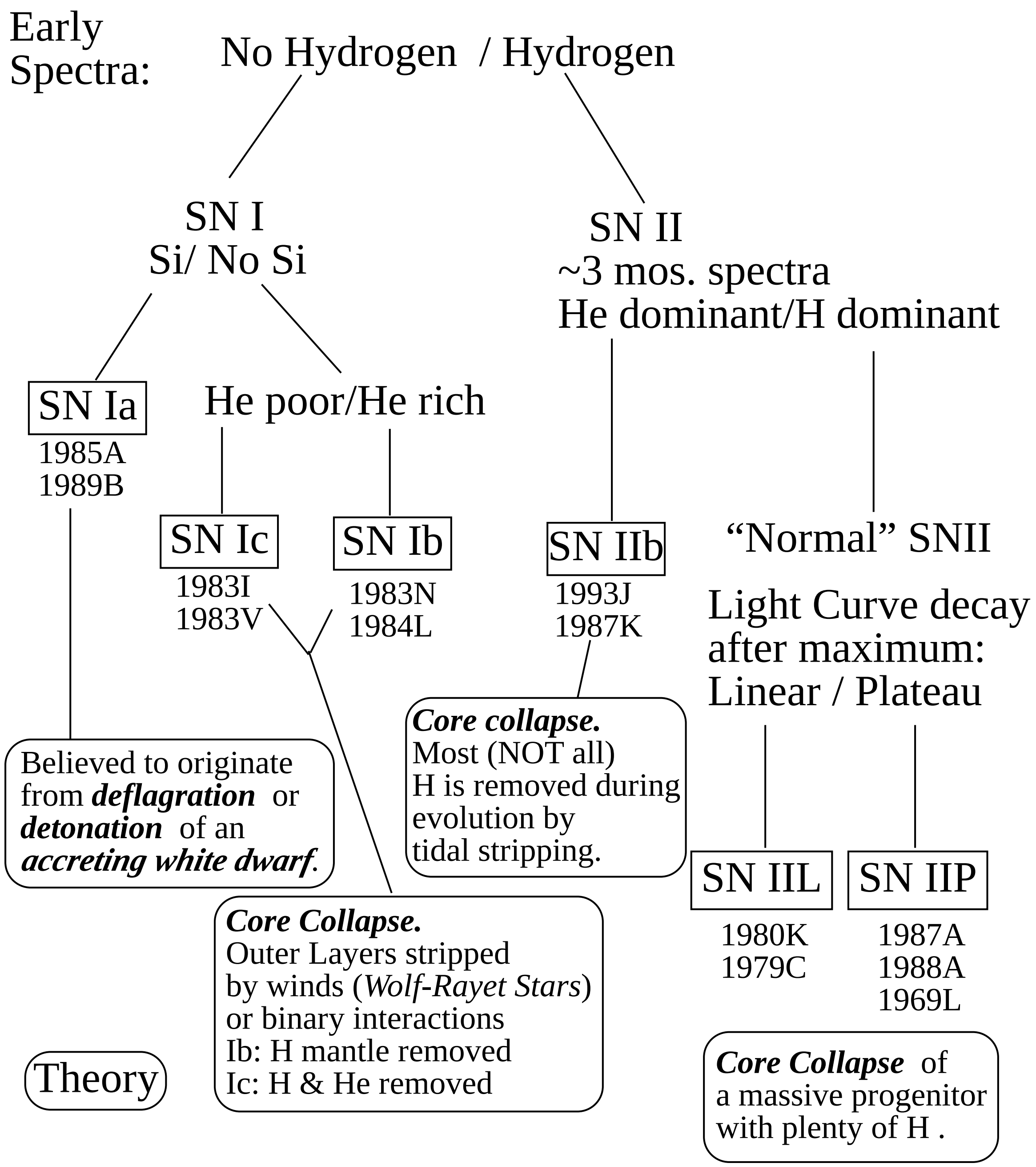

courtesy M.J. Montes

Classifi cation, III

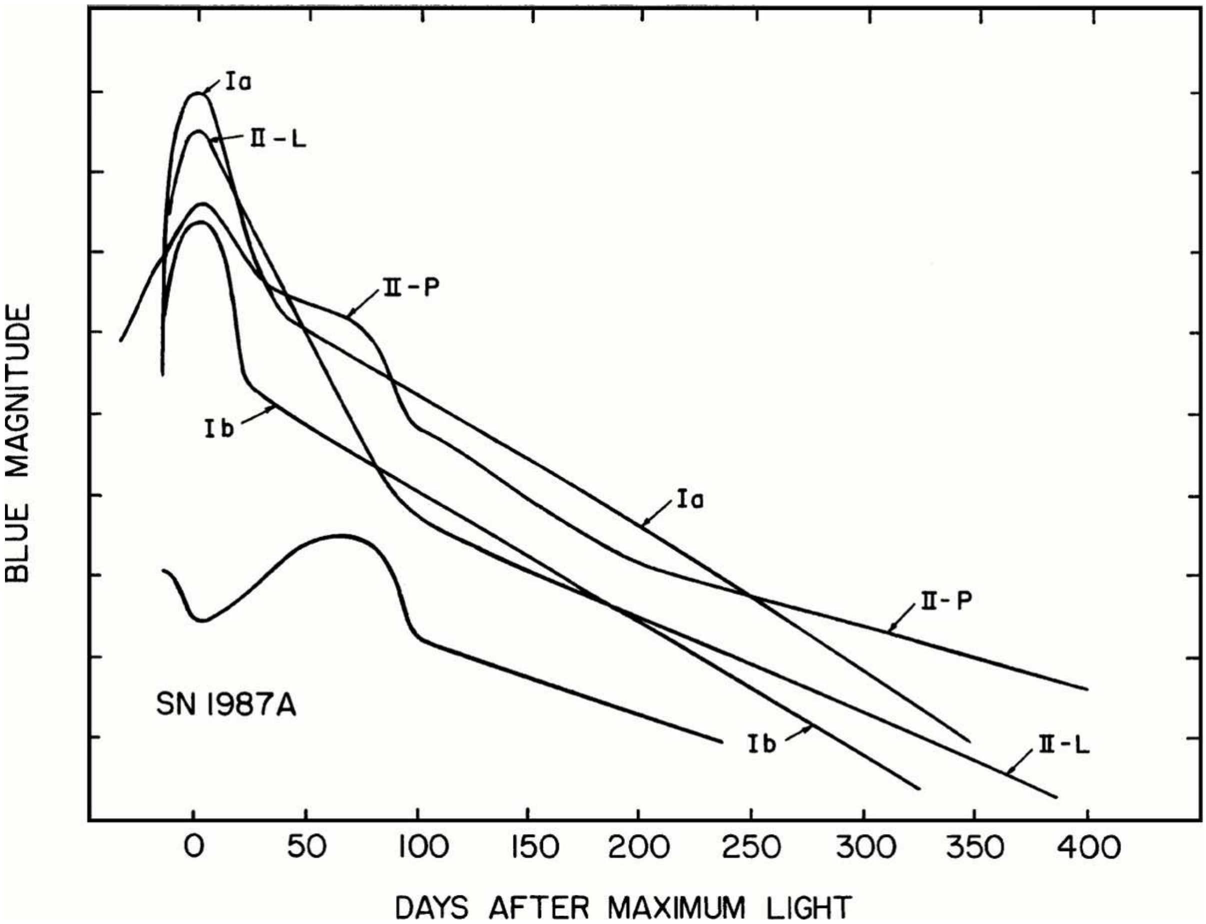

(Filippenko, 1997, Fig. 3)

Light curves of SNe I all very similar, SNe II have much more scatter.

SNe II-L ("linear") resemble SNe I

SNe II-P ("plateau") have const. brightness to within 1 mag for extended period of time.

Models

Clue on origin from supernova statistics:

- SNe II, Ib, Ic: never seen in ellipticals; rarely in S0; generally associated with spiral arms and H II regions.

$\Longrightarrow$ progenitor of SNe II, Ib, Ic: massive stars ($\gtrsim 8\,M_\odot$) $\Longrightarrow$ core collapse

- SNe Ia: all types of galaxies, no preference for arms.

$\Longrightarrow$ progenitor of SNe Ia: accreting carbon-oxygen white dwarfs, undergoing thermonuclear runaway $\Longrightarrow$ lightcurves all very similar $\Longrightarrow$ cosmological standard candles!

SN 1987A

1987 February 23: Explosion of blue supergiant Sandulaek -69°202; closest supernova since Kepler (1604)

courtesy AAO

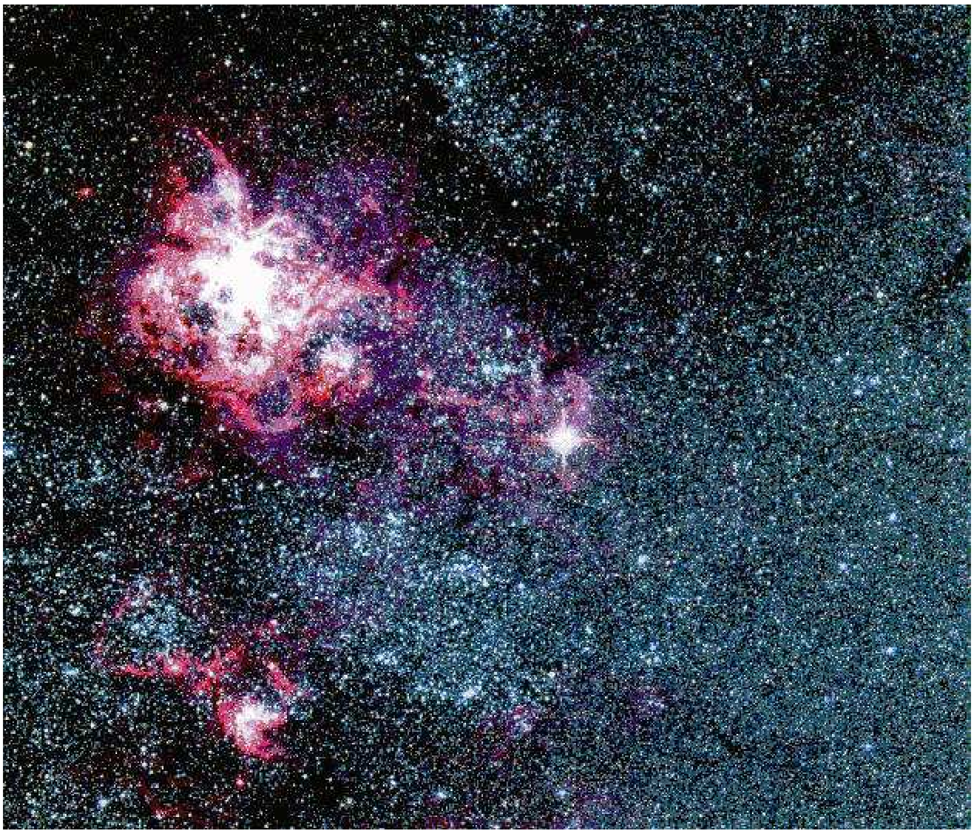

courtesy ESO

IAAT

SN 1987A

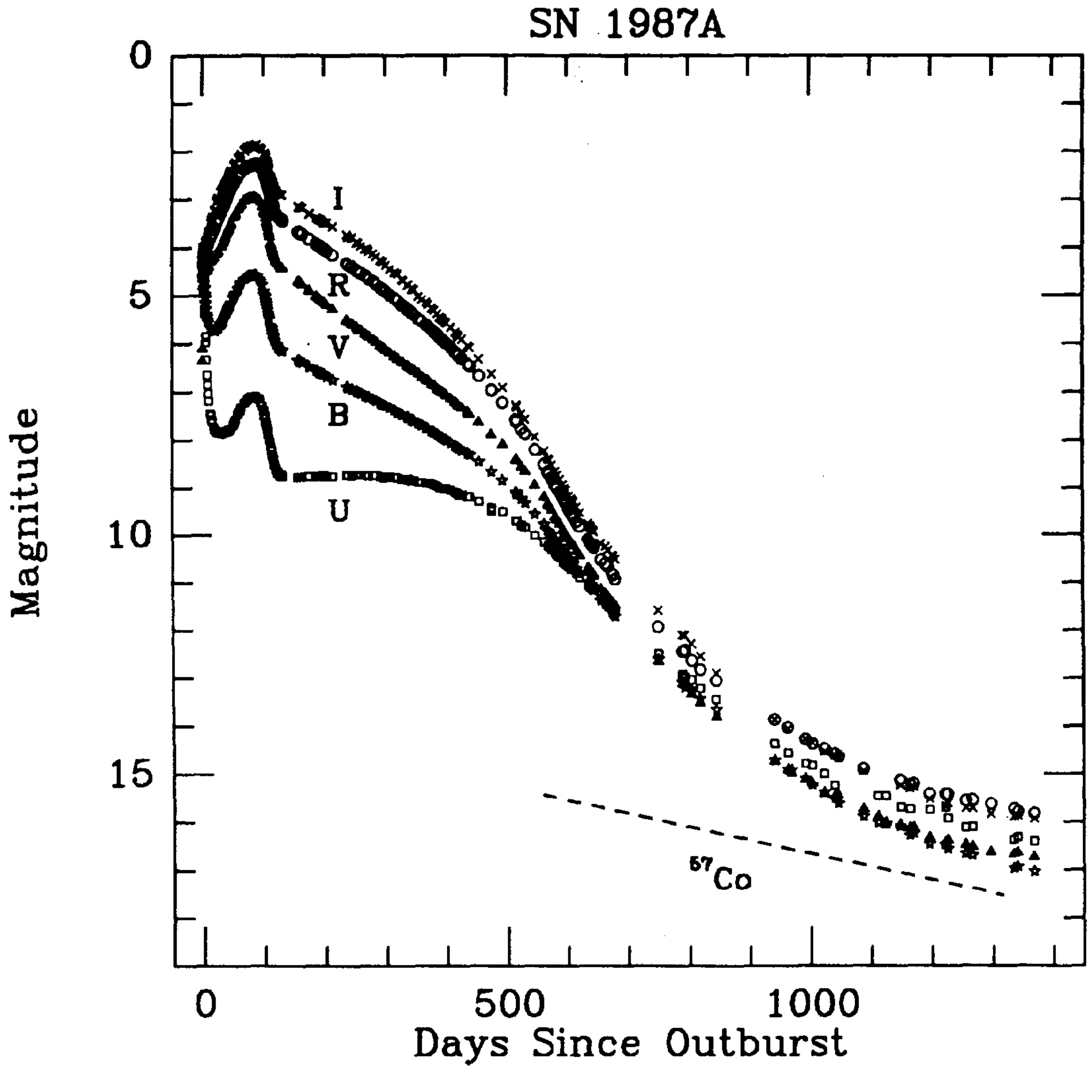

(Suntzeff et al., 1991, Fig. 2)

UVOIR (UV, optical, infrared) light curve resembles SNe II-P, although peak much lower than typical (progenitor was blue supergiant, not red supergiant).

Exponential decay of bolometric luminosity after first few 100 days $\Longrightarrow$ Radioactive decay

SN 1987A

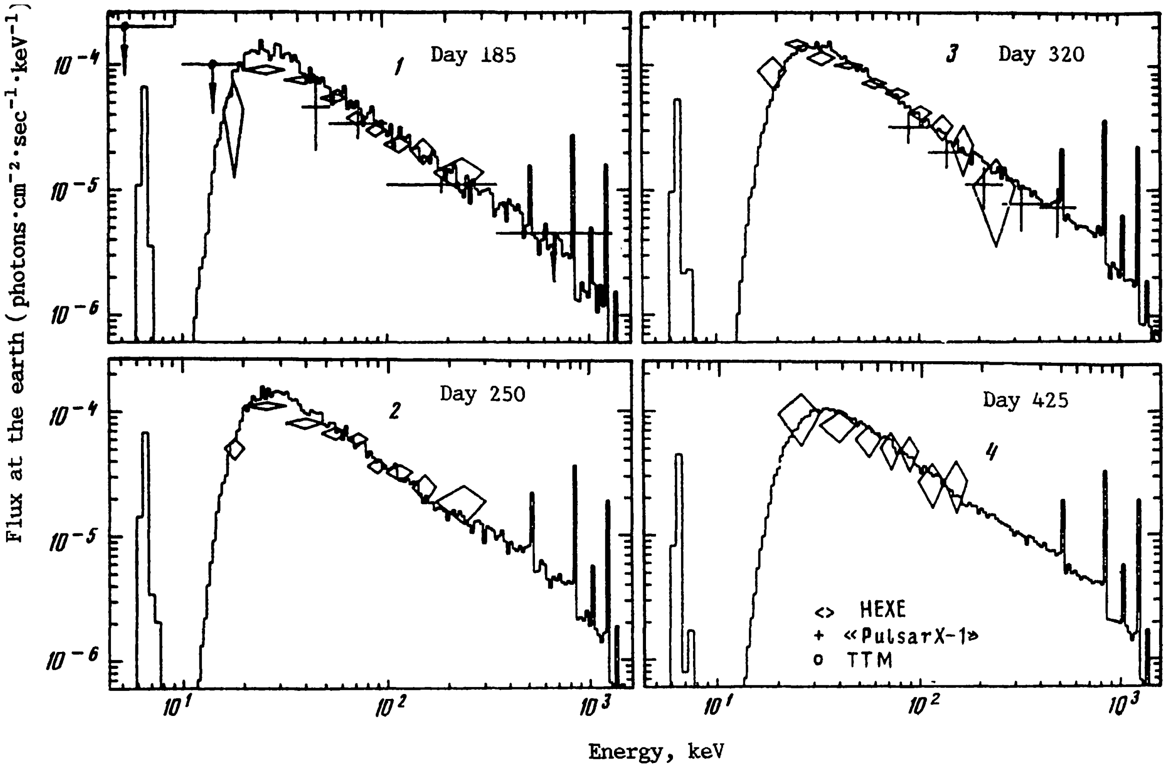

(Sunyaev; 1991)

During SN explosion: formation of ^{56}Ni. Then radioactive decay:

$$^{56}\mathrm{Ni} \xrightarrow[t_{1/2}=6.1\,\mathrm{d}]{\mathrm{EC}} {}^{56}\mathrm{Co} \xrightarrow[t_{1/2}=77.12\,\mathrm{d}]{81\%\mathrm{EC},19\%\beta^+} {}^{56}\mathrm{Fe}$$

Decay: emission of γ-ray lines

Optically thick medium $\Longrightarrow$ downscattering and thermalization $\Longrightarrow$ observed continuum spectrum.

1987: Mir-HEXE: Observed X-ray spectrum agrees with radioactive decay picture.

SN 1987A

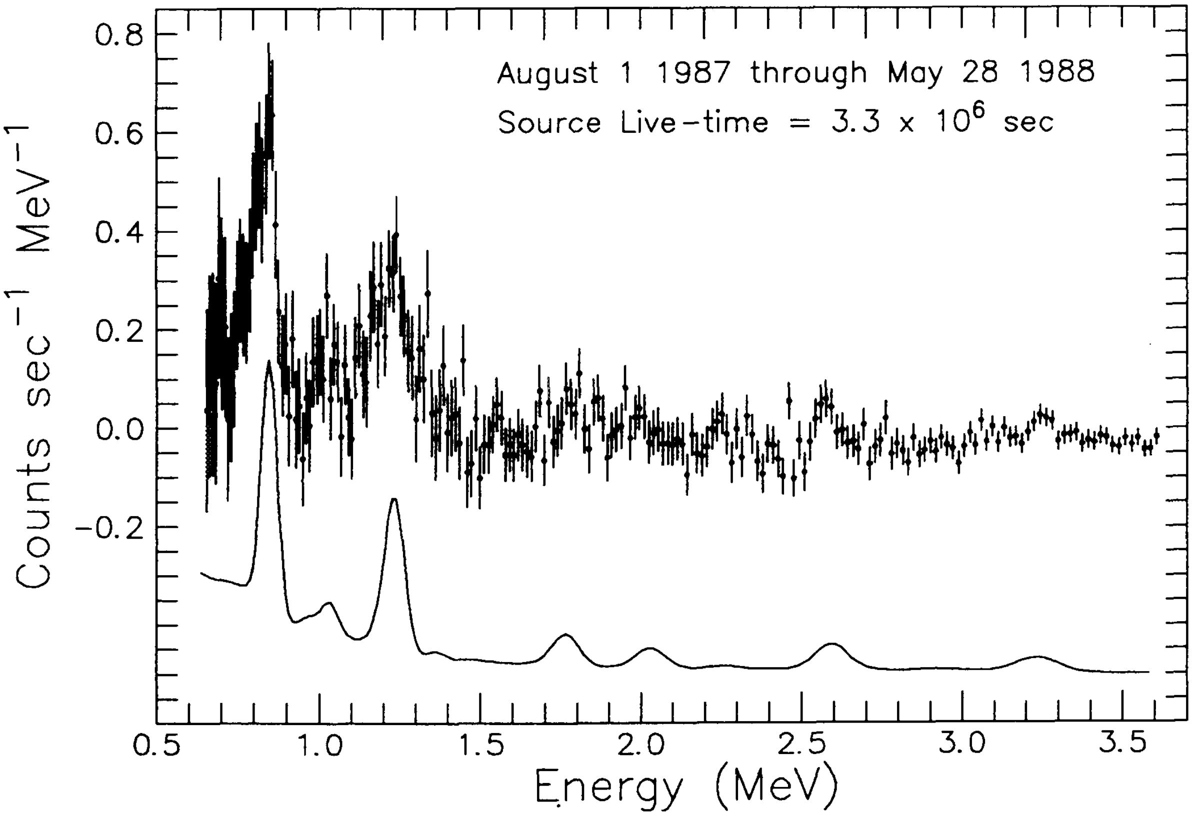

Leising and Share (1990)

Solar Maximum Mission: high resolution γ-ray mission; direct spectroscopy of 847, 1238, 2599, and 3250 keV lines from ^{56}Co decay

SMM finds about 0.07 $M_\odot$ in cobalt.

SN 1987A

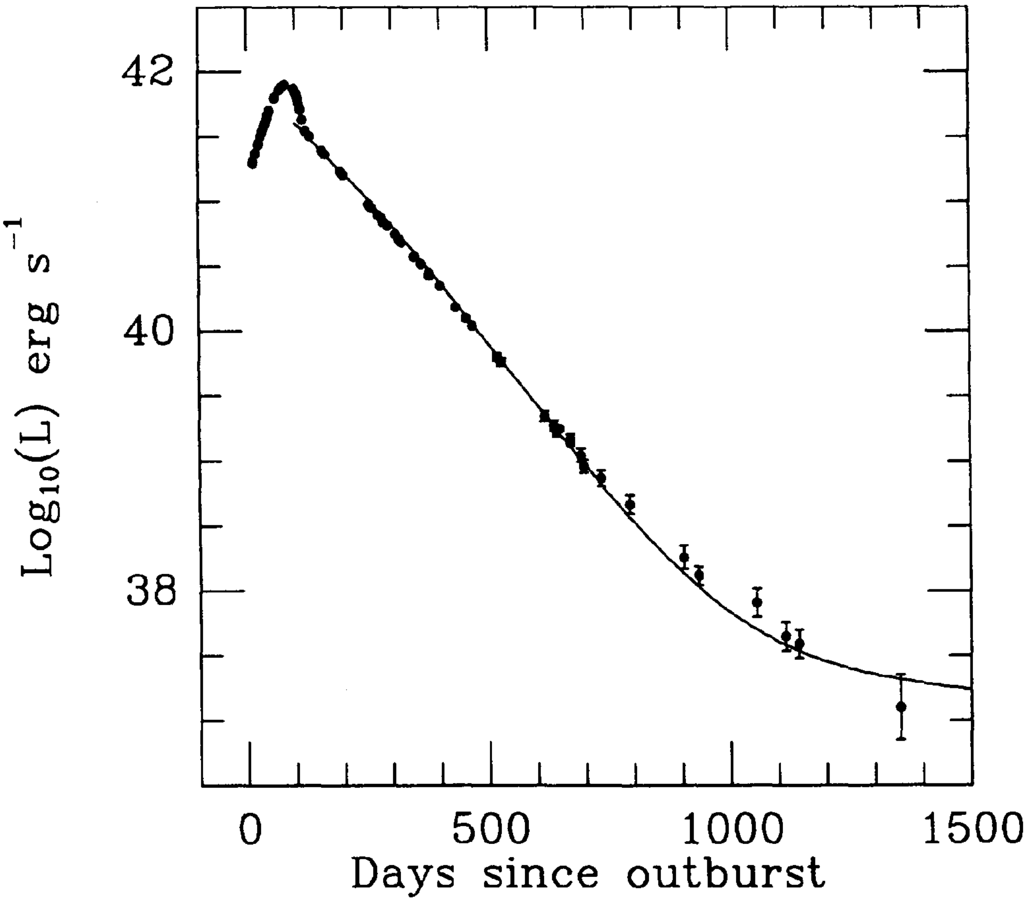

(Co+Ti; Suntzeff et al., 1991, Fig. 9)

Late time light curve due to radioactive decay of Cobalt.

- Day 125–700: dominated by decay of ^{56}Co
- Around day 1000: radioactive decay of ^{57}Co starts to dominate (e-folding time: 391 d).

Optical light curve well described by enhanced ^{57}Co/^{56}Co ratio ($\sim$2.5–4$\times$ solar) plus ^{56}Ni and ^{44}Ti (Suntzeff et al., 1991).

SN 1987A

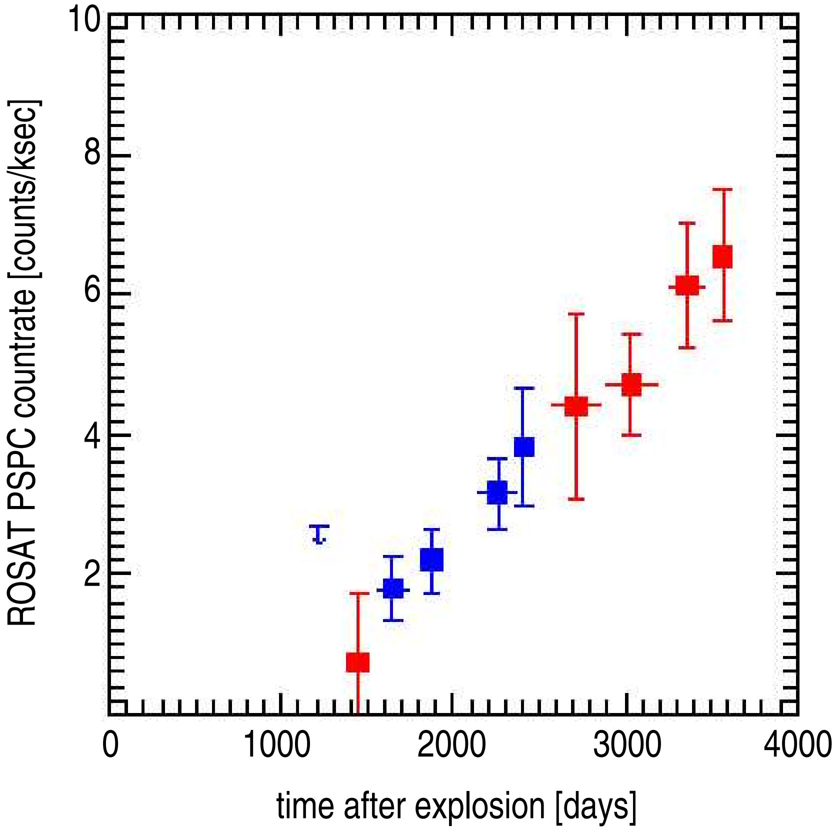

after Hasinger, Aschenbach & Trümper (1996, Fig. 3)

$\sim$1000 d after explosion: the X-ray luminosity of SN 1987A started to brighten again ($L_X \propto t^2$).

Most likely explanation: interaction between SN blast wave and interstellar medium (mainly progenitor stellar wind) $\Longrightarrow$ Supernova remnant!

Introduction, I

After Supernova Explosion: Formation of Supernova Remnant (SNR)

Explosion energy goes into kinetic energy of ejecta:

$$E = \frac{1}{2} M v_{\text{ej}}^2 \qquad (4.1)$$

Therefore

$$v_{\text{ej}} = 10^4\,\text{km}\,\text{s}^{-1} E_{51}^{1/2} \left(\frac{M_{\text{ej}}}{M_\odot}\right)^{-1/2} \qquad (4.2)$$

$$\sim 10^{-2}\,\text{pc}\,\text{yr}^{-1} E_{51}^{1/2} \left(\frac{M_{\text{ej}}}{M_\odot}\right)^{-1/2} \qquad (4.3)$$

where $E_{51} = E/10^{51}\,\text{erg}\,\text{s}^{-1}$.

$\Longrightarrow$ Fast material smashes into stationary ISM

$\Longrightarrow$ shock!

Typical temperatures via thermalization:

$$E \sim NkT = \frac{M}{m_{\text{p}}} kT \quad \Longrightarrow \quad T \sim 10^9\,\text{K} \qquad (4.4)$$

$\Longrightarrow$ X-ray emission!

Introduction, II

Simplifi ed computation if fluid approximation possible, i.e.,

mean free path $\ll$ size of system

Two possible candidates:

1. Ionization length scale
2. Magnetic length scale

Ionization length scale: Need $\sim$50 eV to collisionally ionize hydrogen; cross section: $\sigma_{\text{ion}} \sim a_0^2 \sim 10^{-17}\,\text{cm}^2$. For protons: $10^4\,\text{km}\,\text{s}^{-1} \,\hat{=}\, \sim$2 MeV; assume $n_{\text{H}} = 1\,\text{cm}^{-3}$

$\Longrightarrow$ typical stopping length:

$$l_{\text{ion}} \sim \frac{\text{Energy}}{\text{E Loss/Ionization}} \cdot \text{mfp btw collisions} \tag{4.5}$$

$$\sim \left(\frac{2\,\text{MeV}}{50\,\text{eV}}\right) \frac{1}{n_{\text{H}}\sigma_{\text{ion}}} \sim 10^3\,\text{pc} \tag{4.6}$$

$\Longrightarrow$ l_{ion} is too large

Magnetic length scale given by Larmor radius ($B \sim 3\,\mu$G)

$$R_{\text{L}} = \frac{qB}{mc} \sim 2 \times 10^{10}\,\text{cm} \sim 10^{-8}\,\text{pc} \tag{4.7}$$

$\Longrightarrow$ R_{L} is small enough

Use fluid approximation to study SNR evolution!

Introduction, III

Generally, four phases of SNR evolution:

Free expansion : velocity very large with respect to ambient medium, swipe up large fraction of the medium

Sedov phase : Expansion driven by conversion of internal energy into kinetic energy

Snowplough phase : energy loss due to radiative cooling becomes important, shock becomes isothermal, shell moves with constant radial momentum (“snow plough”).

Merging phase : speed of expansion $<$ speed of sound, SNR dissolves into ISM

Will now look at these phases in detail.

Free Expansion, I

Free Expansion: Material moves with uniform velocity, $r \propto t$.

Possible until sweptup mass $\sim$ ejected mass:

$$M_{\text{sweptup}} \sim \frac{4\pi}{3}\rho_{\text{ISM}} r_f^3 = M_{\text{ej}} \quad (4.8)$$

(assuming constant density around SN)

Therefore

$$r = \left(\frac{3}{4\pi}\right)^{1/3} M^{1/3}\rho^{-1/3} \quad (4.9)$$

$$= 2\,\text{pc} \left(\frac{M_{\text{ej}}}{M_\odot}\right)^{1/3} \left(\frac{\rho_{\text{ISM}}}{2\times 10^{-24}\,\text{g}\,\text{cm}^{-3}}\right)^{-1/3} \quad (4.10)$$

Corresponding time scale

$$t \sim \frac{r}{v_{\text{ej}}} \sim 200\,\text{yr} \left(\frac{M_{\text{ej}}}{M_\odot}\right)^{5/6} E_{51}^{-1/2}\rho_{24}^{-1/3} \quad (4.11)$$

(using Eq. 4.2).

SN 1987A is only close remnant in free expansion phase.

IAAT

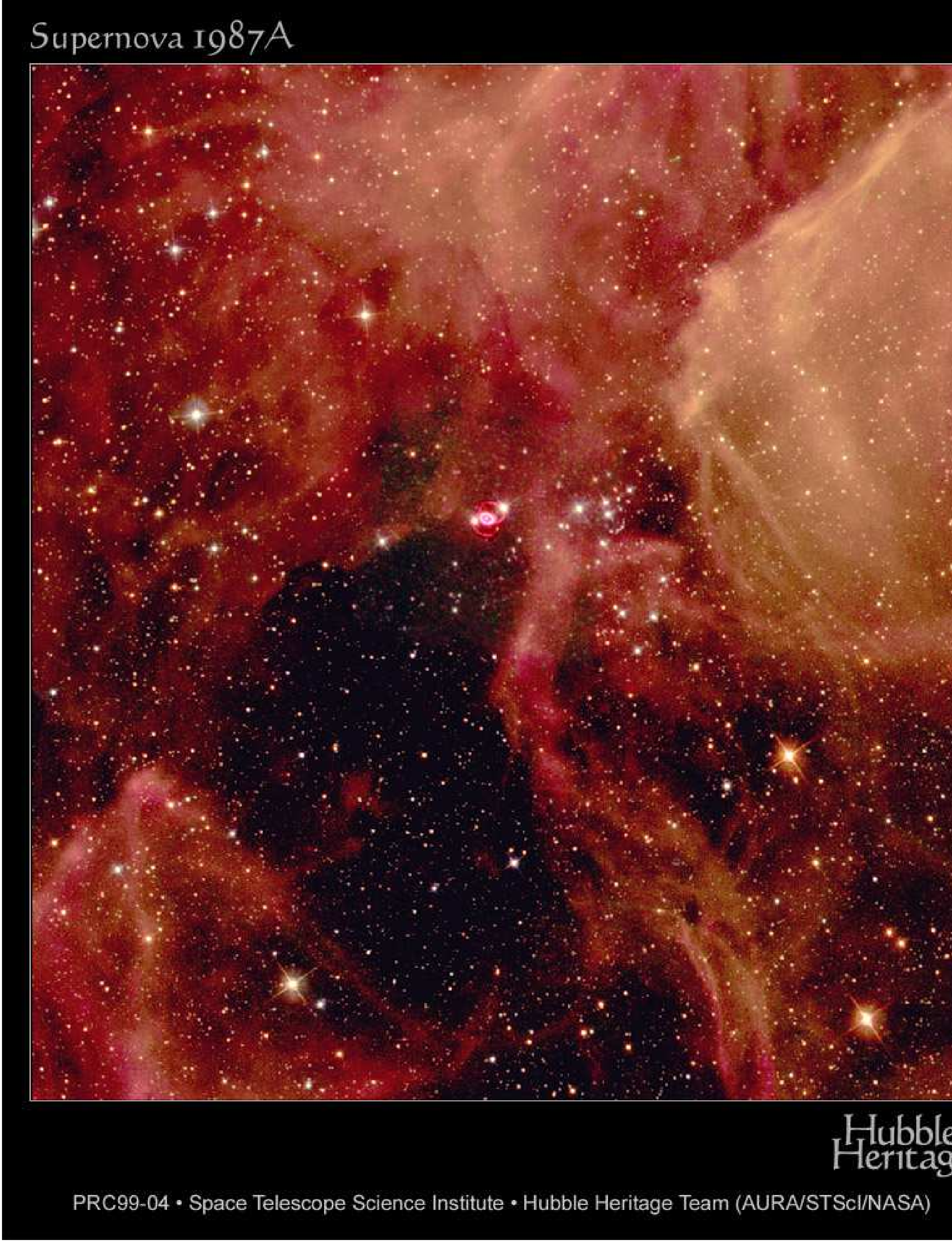

Two features currently seen: central ring due to impact of blast wave on circumst
material and outer rings, possibly due to ionization of material illuminated by SN b
Material possibly from bipolar outflow during blue supergiant phase (fast blue
wind colliding with slower RG wind); material ejected $\sim$20000 years before explos

Free Expansion, III

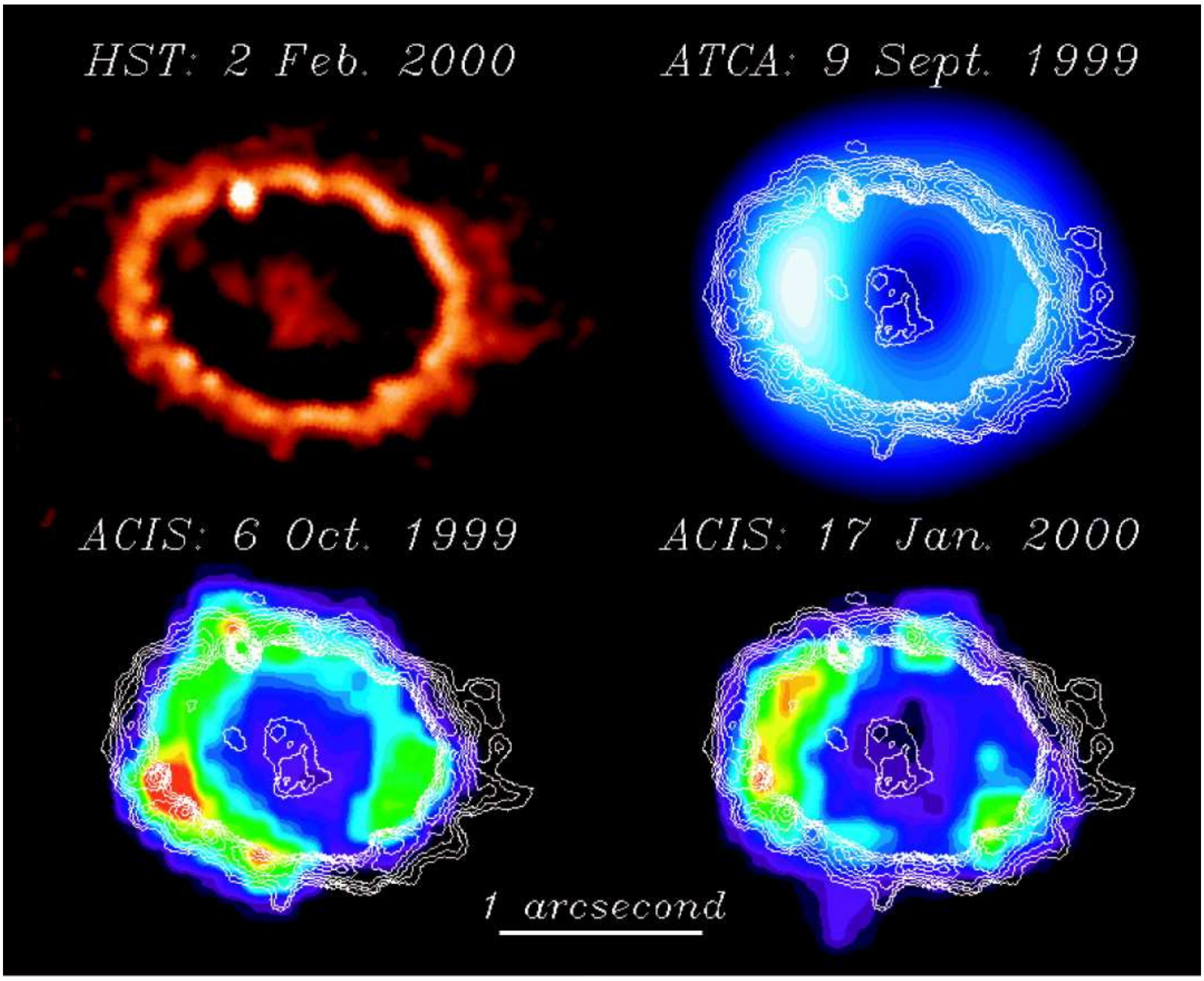

(Burrows et al., 2000, Fig. 1)

Ring ($1.66'' \times 1.21''$) around SN 1987A from shock heating at point of first contact between blast wave and equatorial ring from stellar wind of progenitor. Mainly ionized C and N.

Bright spots brightened first (1997) $\Longrightarrow$ “bullets” within faster than normal blast wave; 2000: many more spots $\Longrightarrow$ rest of blast wave has reached location of ring.

Sedov Phase, I

After free expansion: further energy for expansion comes from internal energy of system, such that total energy stays roughly constant (adiabatic expansion) $\Longrightarrow$ Sedov phase or blast wave phase.

Energy constancy translates to

$$E \sim \underbrace{\frac{1}{2}\left(\frac{4\pi}{3}\right)\rho r^3 v^2}_{\text{kinetic energy}} + \underbrace{A\left(\rho v^2\right)\left(\frac{4\pi}{3}\right) r^3}_{\text{internal energy}} \tag{4.12}$$

$$\propto \rho r^3 v^2 \overset{!}{=} \text{const.} \tag{4.13}$$

where A is a constant. Solving for $v = \mathrm{d}r/\mathrm{d}t$:

$$\frac{\mathrm{d}r}{\mathrm{d}t} \propto \left(\frac{E}{\rho}\right)^{1/2} r^{-3/2} \tag{4.14}$$

Separation of variables gives

$$r \propto \left(\frac{E}{\rho}\right)^{1/5} t^{2/5} \tag{4.15}$$

Detailed theory (Padmanabhan, Vol. 1, Sec. 8.12) shows that the constant of proportionality is ~ 1 for $\gamma = 5/3$.

Note that these equations assume $\rho =$ const., which is not true since remnant expands; still, good enough for order of magnitude computations.

Sedov Phase, II

Inserting numbers into Eq. (4.15) gives:

Radius of the shell:

$$r \approx \left(\frac{E}{\rho}\right)^{1/5} t^{2/5} \sim 0.3\,\mathrm{pc}\, E_{51}^{1/5} n_{\mathrm{H}}^{-1/5} t_{\mathrm{yr}}^{2/5} \tag{4.16}$$

Velocity of the shell:

$$v = \dot{r} = \frac{2}{5}\left(\frac{E}{\rho}\right)^{1/5} t^{-3/5} \tag{4.17}$$

Solving Eq. (4.16) for t and inserting

$$= \frac{2}{5}\left(\frac{E}{\rho}\right)^{1/5} r^{-3/2}\left(\frac{E}{\rho}\right)^{3/10} \tag{4.18}$$

$$\sim 5000\,\mathrm{km\,s^{-1}}\left(\frac{r}{2\,\mathrm{pc}}\right)^{-3/2} E_{51}^{1/2} n_{\mathrm{H}}^{-1/2} \tag{4.19}$$

Temperature of the shell follows from assuming thermalization, i.e., $m_{\mathrm{p}}v^2/2 = NkT$ ($\Longrightarrow T \propto v^2$):

$$T \sim 6 \times 10^8\,\mathrm{K}\left(\frac{r}{2\,\mathrm{pc}}\right)^{-3} E_{51} n_{\mathrm{H}}^{-1} \tag{4.20}$$

$$\sim 10^6\,\mathrm{K}\, E_{51}^{2/5} n_{\mathrm{H}}^{-2/5}\left(\frac{t}{3\times 10^4\,\mathrm{yr}}\right)^{-6/5} \tag{4.21}$$

Measuring r, v, and T allows to determine age of supernova remnant.

Mainly bremsstrahlung emission with $T \sim 10^6\,\mathrm{K} \Longrightarrow$ X-ray emission!

Sedov Phase, III

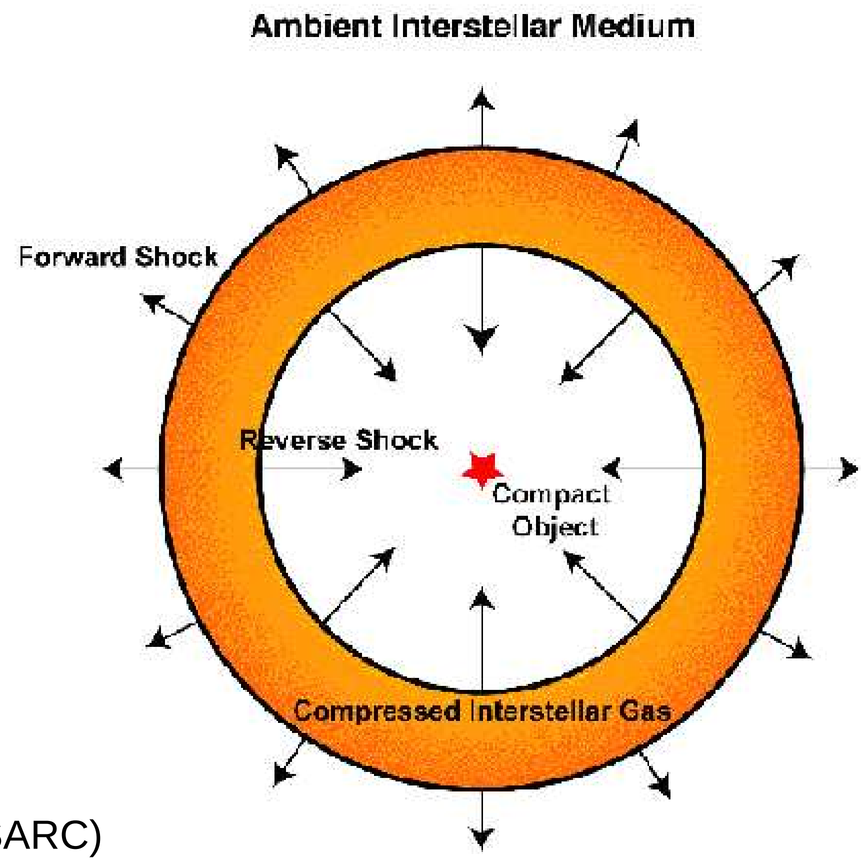

(HEASARC)

Nature of shock: "contact discontinuity":

forward shock outside of whichISM has not yet reacted to SN blast wave

reverse shock where information from ISM has traveled backwards into SN ejecta

Between two shocks ($\delta r \sim 25\%$): hot material.

These remnants are called shell-like remnants.

Note: limb-brightening due to shell-structure (longer path through bright edge $\Longrightarrow$ ring)

Sedov Phase, IV

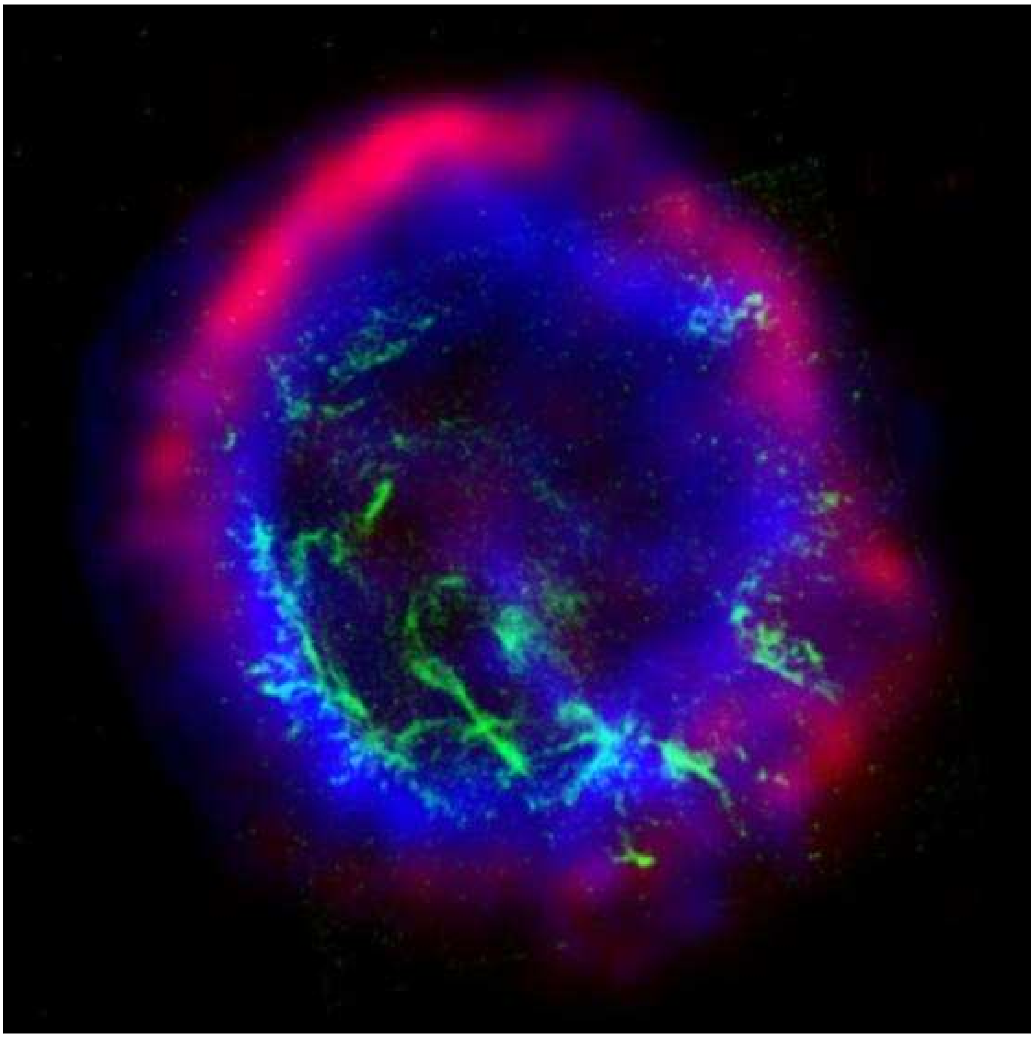

E0102−72.3; blue: X-rays (Chandra), red: radio (ATCA), green: optical (HST)

Best example for contact discontinuity:

E0102−72.3:

forward shock bright in radio emission

reverse shock bright in X-ray emission

Optical emission only visible as optical fi laments.

Sedov Phase, V

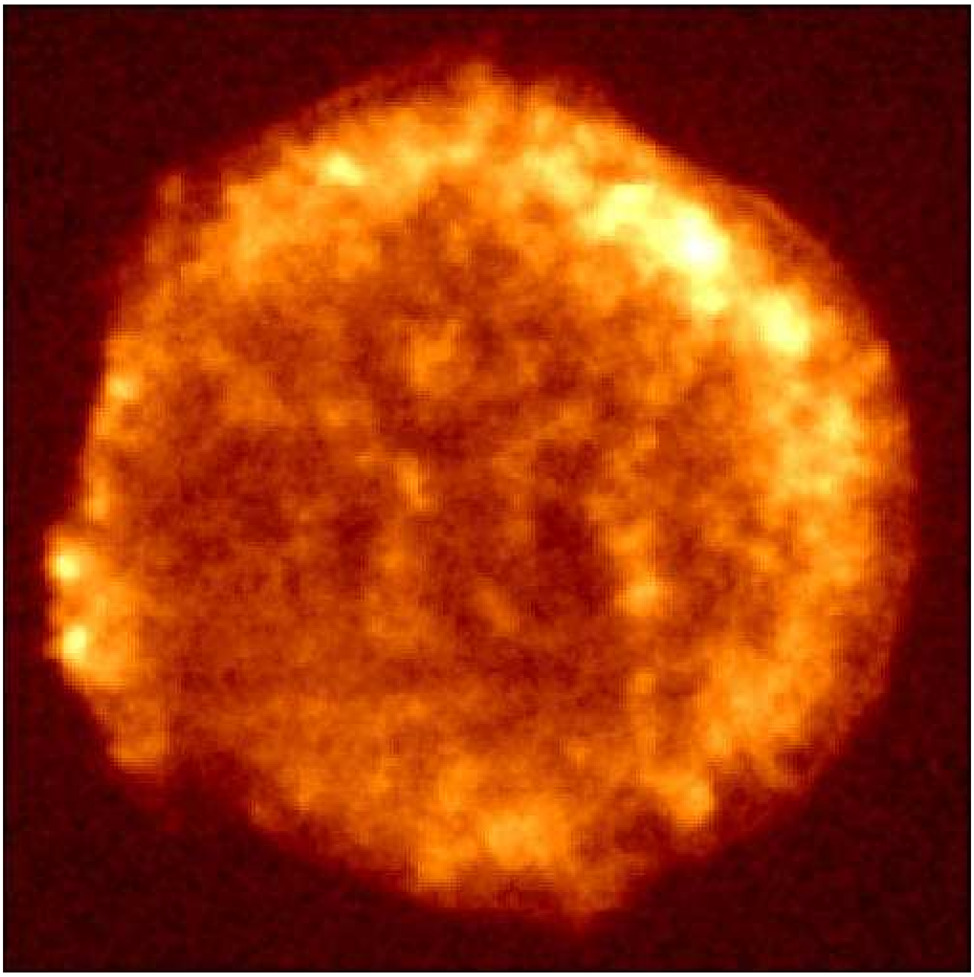

ROSAT HRI; courtesy J. Hughes

Tycho's supernova remnant: 1572 November 11, first naked eye supernova for a long time, now very difficult to see in optical.

Brahe, De Stella Nova

Sedov Phase, VI

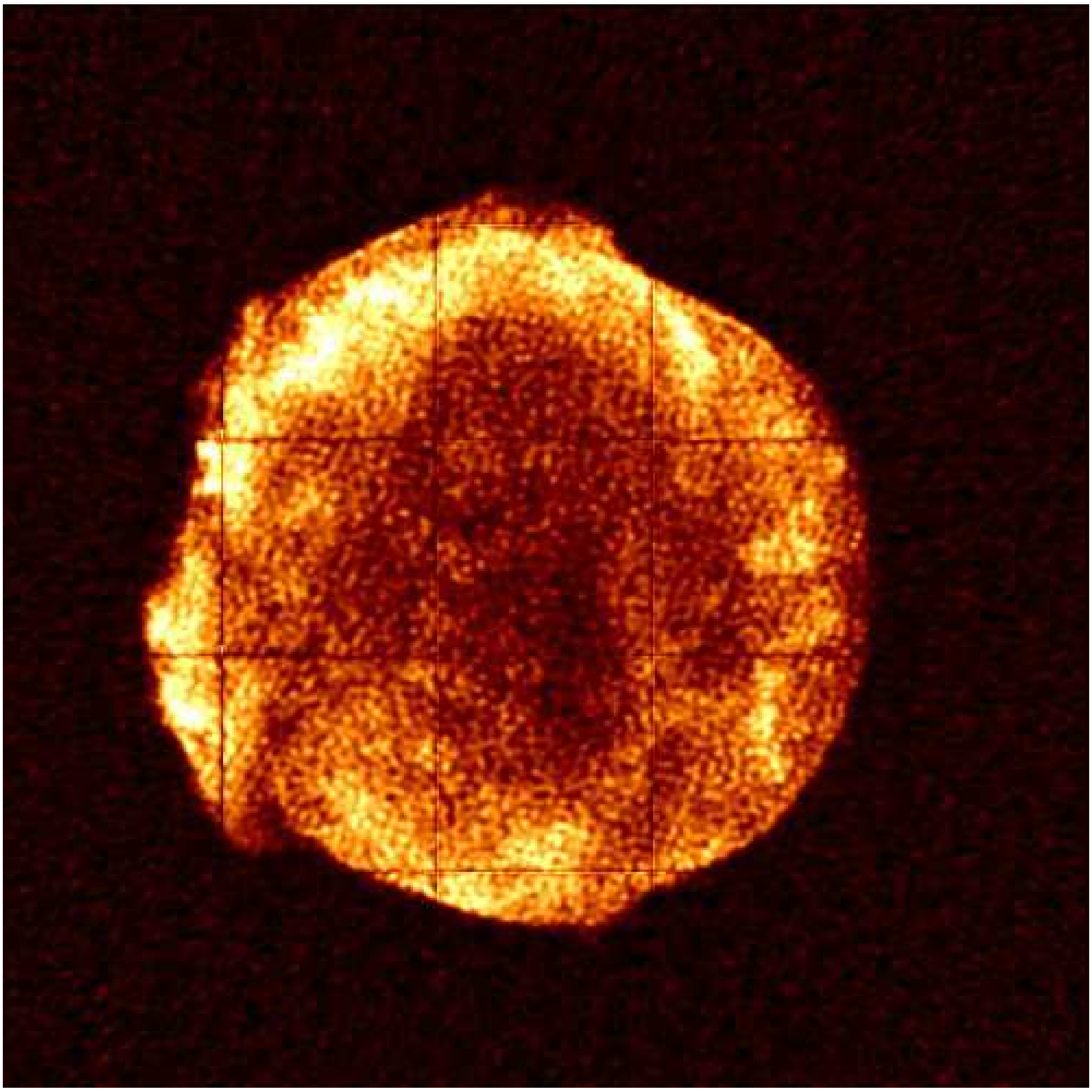

Tycho's SNR, VLA, 0.33 MHz (diameter 7 pc; courtesy F. Lazio)

Tycho is also bright in the radio.

B-field frozen into plasma $\Longrightarrow$ shock produces high B-field regions $\Longrightarrow$ emission of synchrotron radiation

Sedov Phase, VII

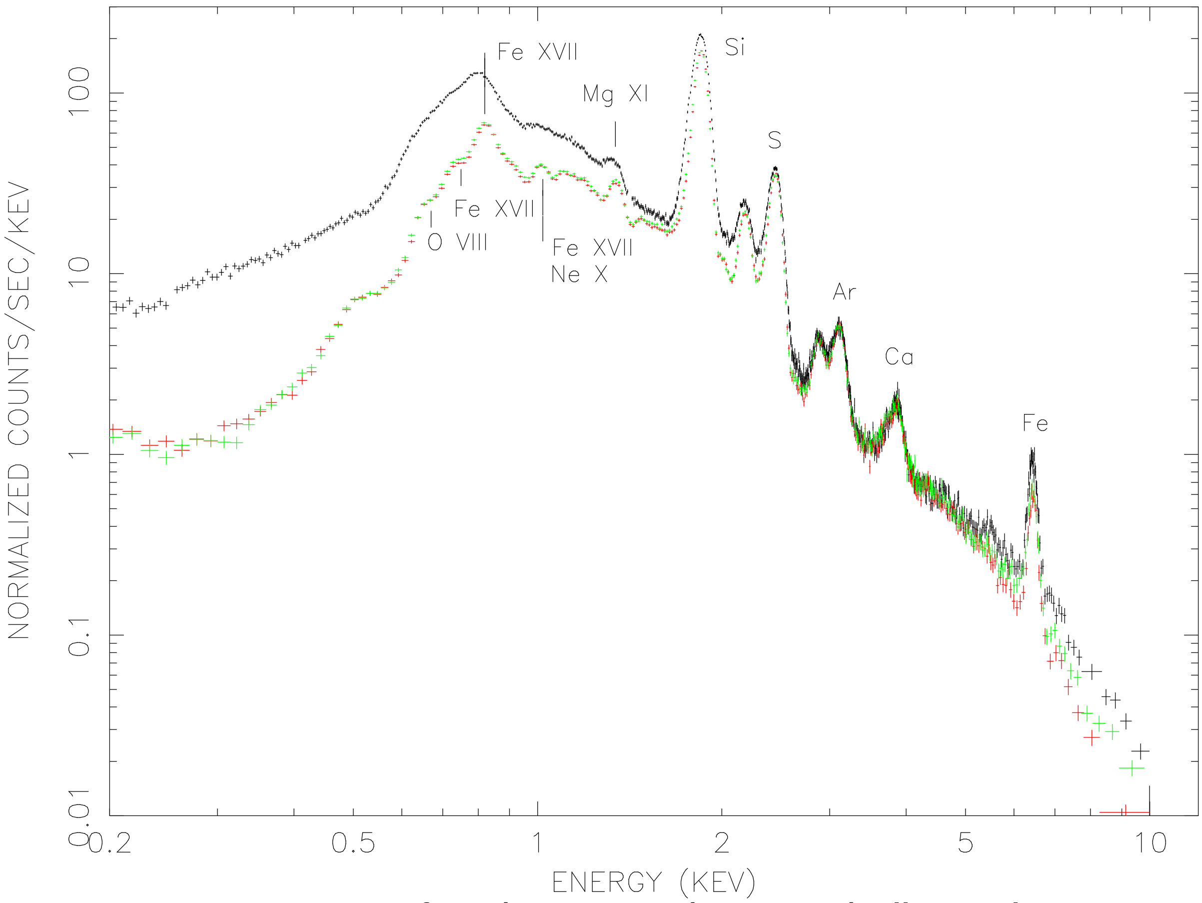

XMM EPIC spectrum of Tycho's SNR (Decourchelle et al., 2001, Fig. 1a)

X-ray spectrum is line dominated $\Longrightarrow$ line emission from shock excited plasma.

Mass estimate from X-ray spectroscopy and radio: 1...2 $M_\odot$ $\Longrightarrow$ ~1.4 $M_\odot$?!?
$\Longrightarrow$ remnant of type I explosion?

Sedov Phase, VIII

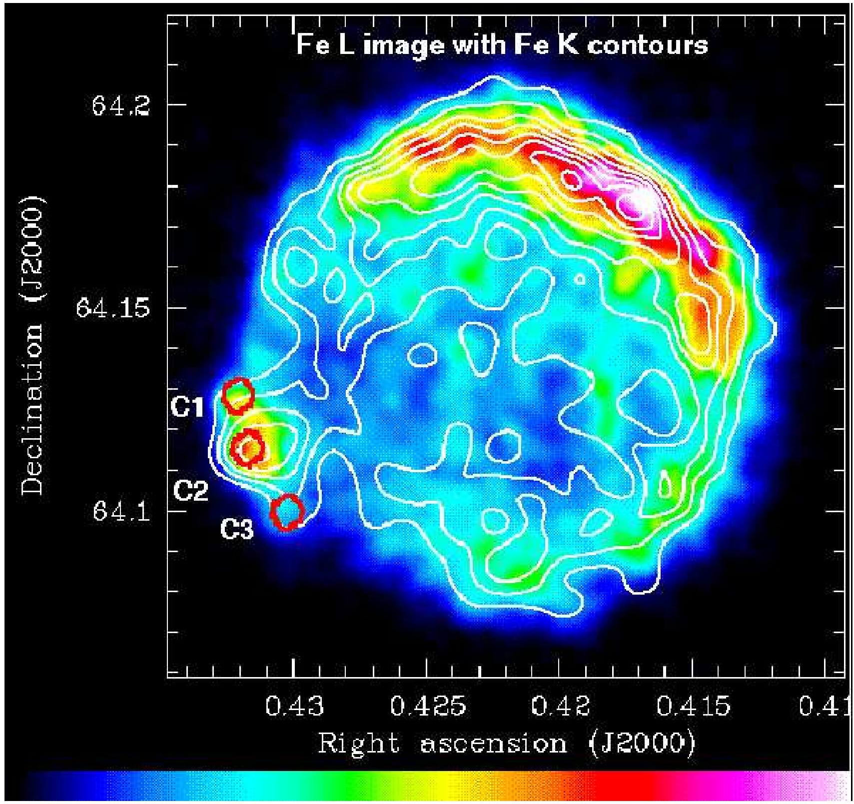

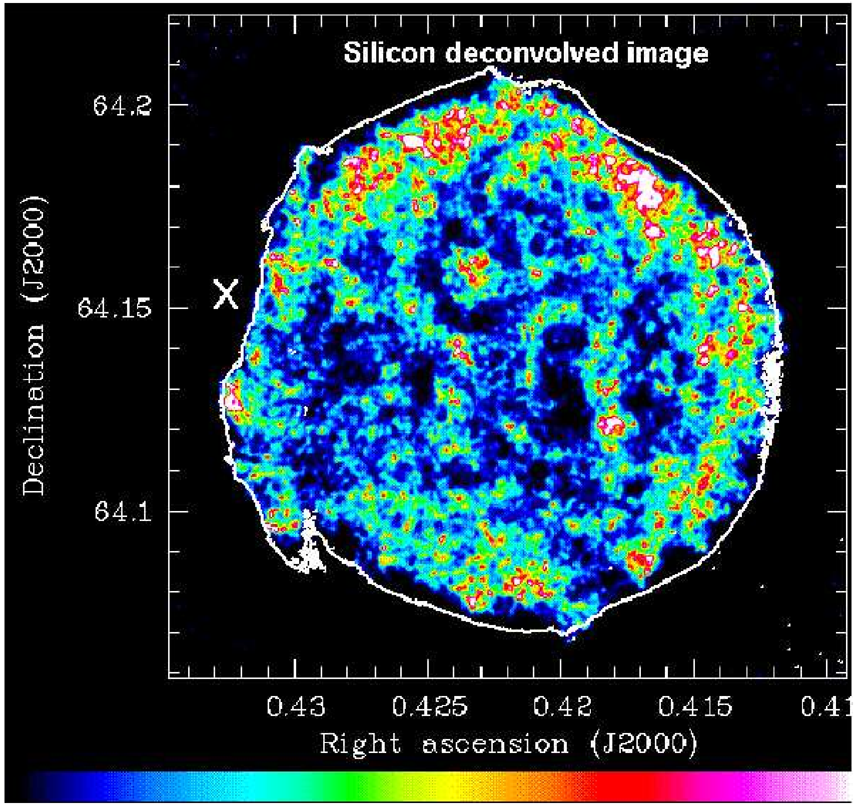

Tycho; XMM-Newton EPIC; Decourchelle et al., 2001

X-ray spectroscopy allows mapping of element distribution in remnant
$\Longrightarrow$ structure of progenitor.

Sedov Phase, IX

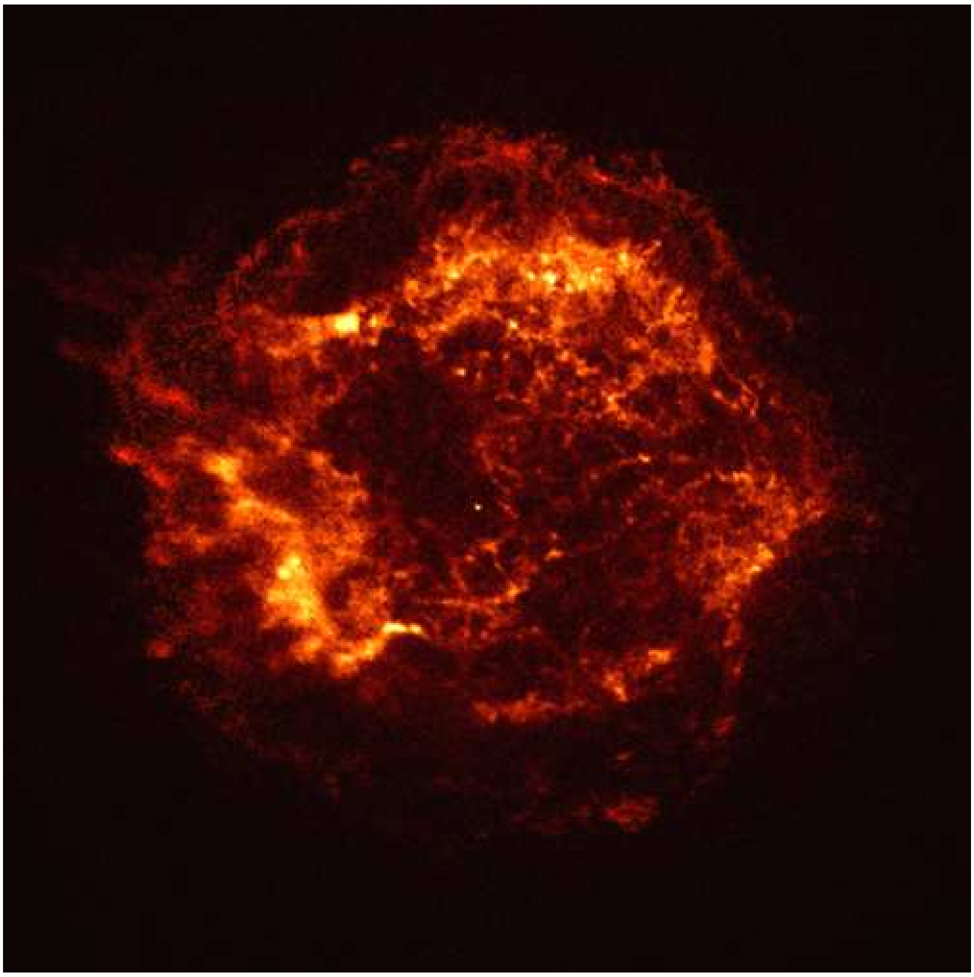

Cas A Chandra fi rst light

Cassiopeia A: Young remnant (∼1670), no optical explosion observed
Mass of ejected material 10–15 $M_\odot$ $\Longrightarrow$ possibly type II?

Type II are also fainter, explaining why explosion has not been reported.

2000: Chandra discovers point-source in center $\Longrightarrow$ neutron star $\Longrightarrow$ confirming type II assumption!

Sedov Phase, X

A Chandra portfolio of Cas A:

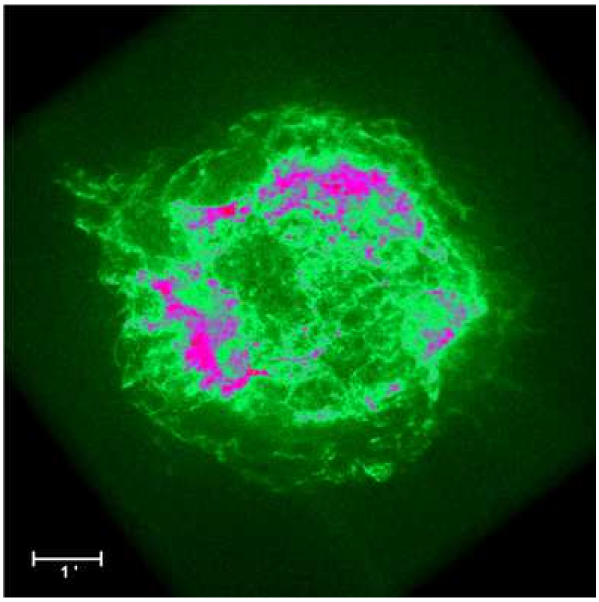

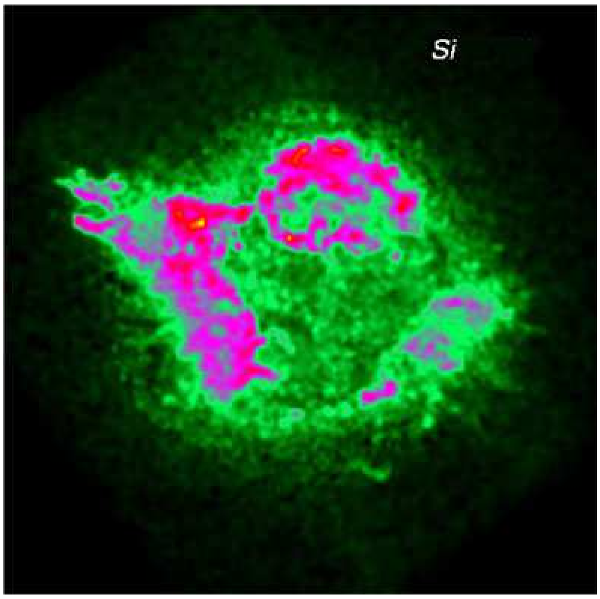

broad band

Silicon

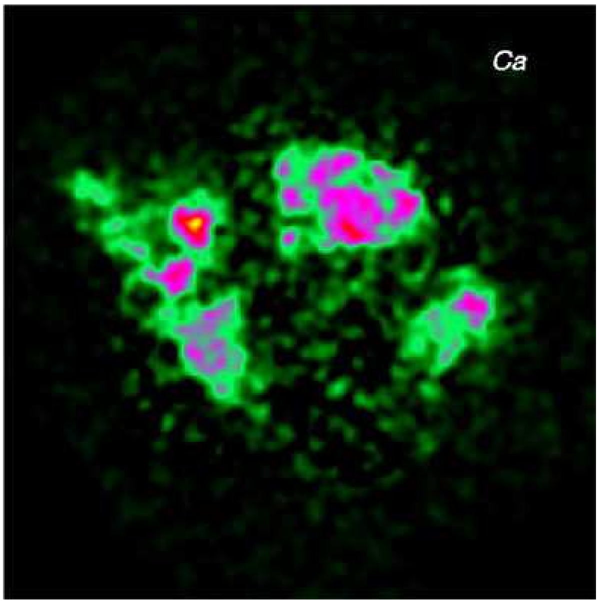

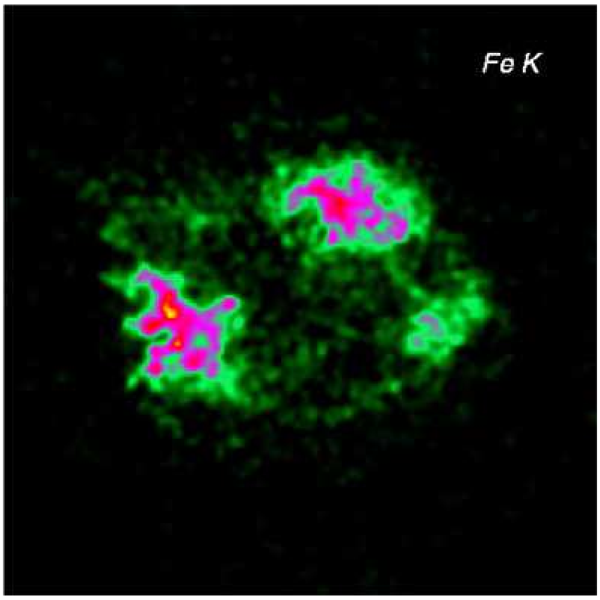

Calcium

Iron

Sedov Phase, XI

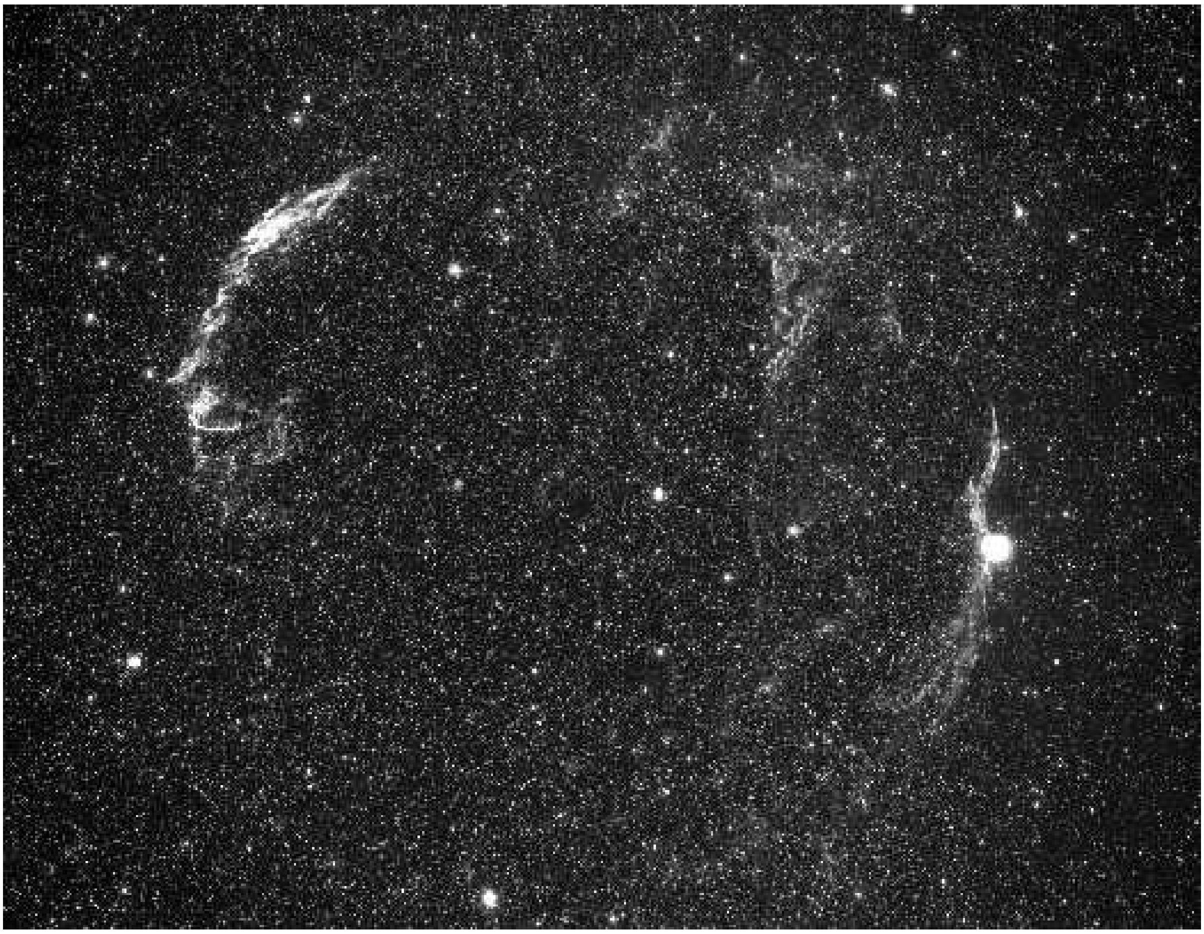

Cygnus Loop (diameter $\sim 2.5^\circ$; optical; Wallis/Provin)

Cygnus loop/Veil nebula: end of Sedov phase ($r \sim 20$ pc, $v \sim 115$ km s^{-1}, estimated age $t \sim 20000$ yr)

Interior ($<$18 pc) empty of material (swept free by progenitor wind).

Sedov Phase, XII

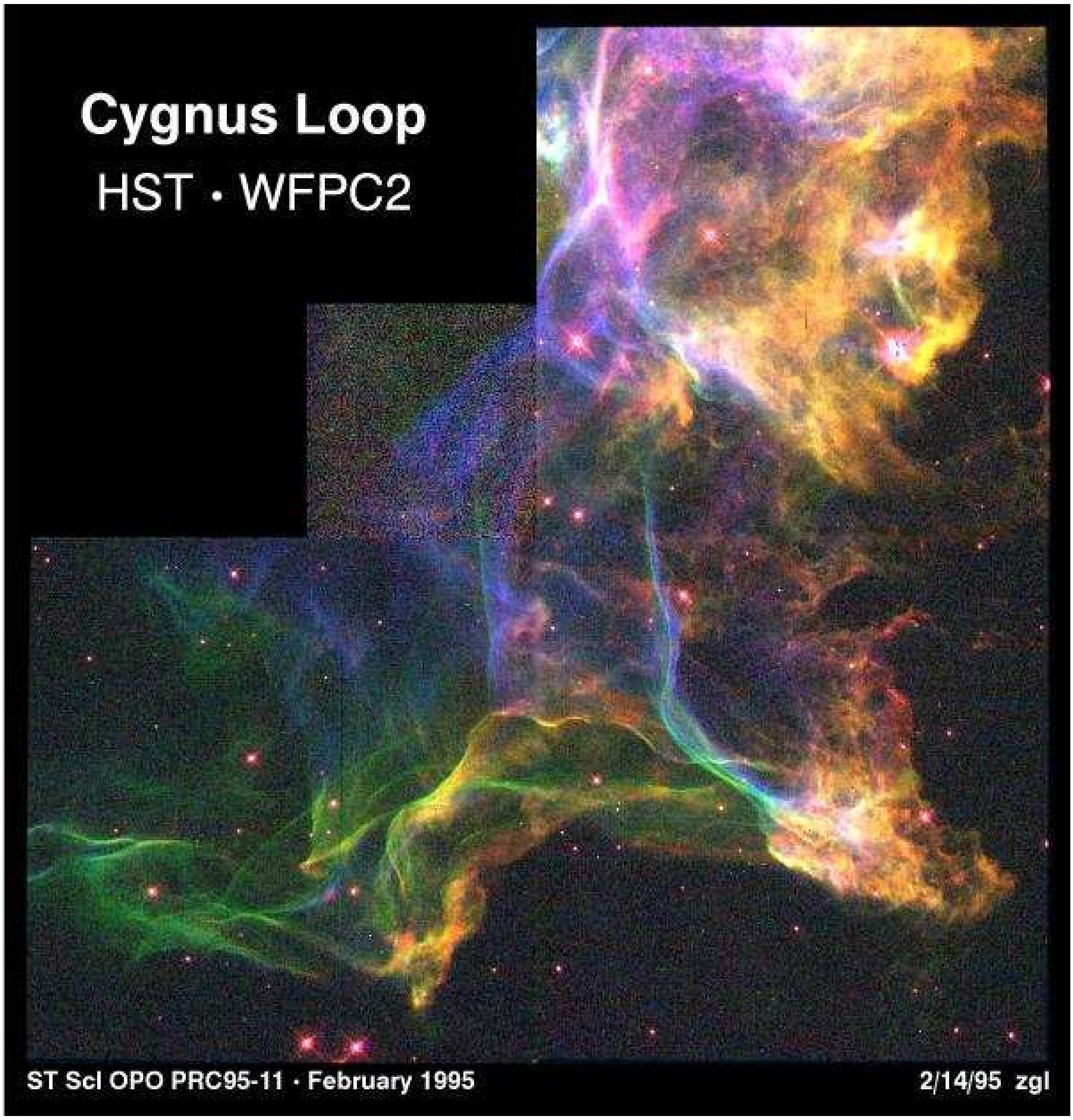

light shocked ISM gas on top of dense gas;
deceleration of gas as effective gravity $\Longrightarrow$
Rayleigh Taylor instability!

Sedov Phase, XIII

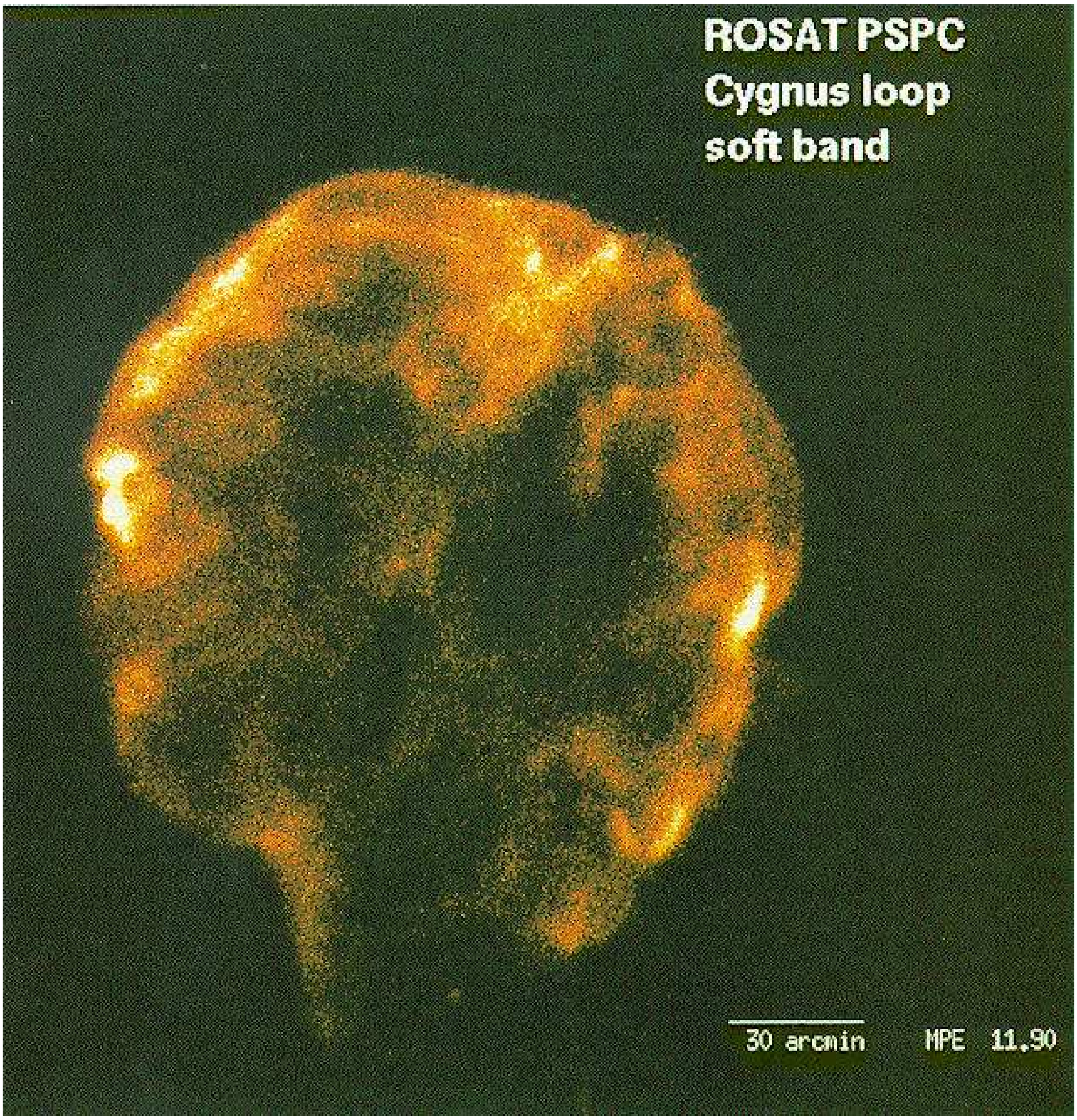

Fit to observations:
inner temperature: 3×10^6 K,
initial energy release $\sim 3 \times 10^{50}$ erg,
100 $M_\odot$ within shell.

Note breakup in southern part of nebula; low density region in ISM?

Sedov Phase, XIV

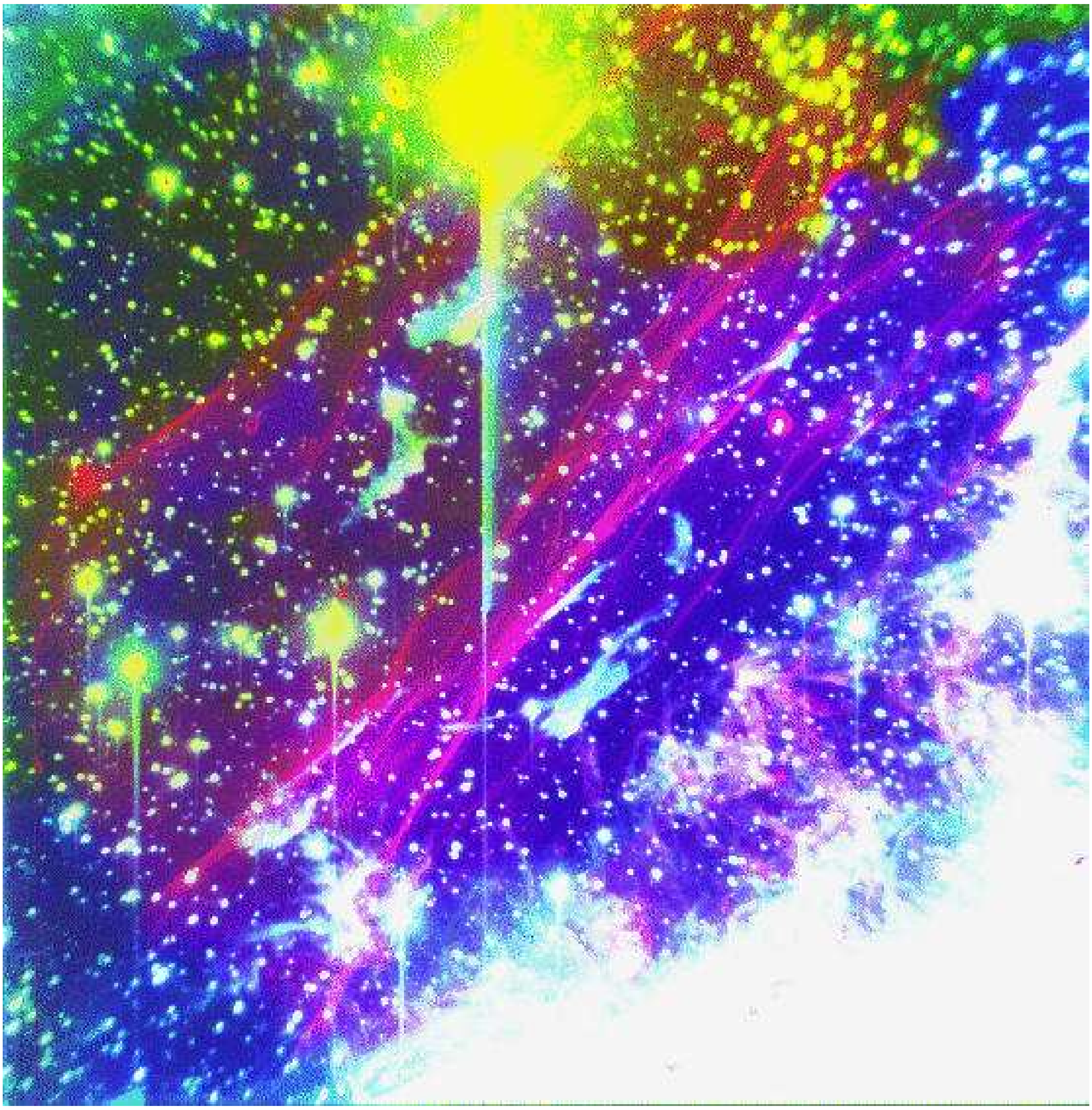

optical/X-ray composite of Cygnus loop (Hester et al., 1994)
blue: X-ray (ROSAT); red: Hα; green: O III.

Optical filaments due to compressed interstellar clouds.

Snow-plough Phase, I

End of Sedov phase when energy cannot be conserved.
Shock continues with its intrinsic momentum, "ploughing" through ISM $\Longrightarrow$ snowplough phase or radiative phase.

Major source of energy loss: Radiative cooling.
Here: collisional excitation and radiative recombination
$\Longrightarrow$ coronal plasma (see chapter 2).

> During snowplough phase, strong optical line emission, mainly from filaments in rim of SNR with temperature $T \sim 10^4$ K; only weak X-ray emission

Cooling function Λ:

$$n_\mathrm{H}^2 \Lambda(T) \approx 10^{-22}\,\mathrm{erg\,cm^3\,s^{-1}}\, n_\mathrm{H}^2 T_6^{-1/2} \tag{4.22}$$

cooling timescale:

$$t_\mathrm{cool} \approx \frac{nkT}{n^2\Lambda(T)} \sim 4 \times 10^4\,\mathrm{yr}\, \frac{T_6^{3/2}}{n_\mathrm{H}} \tag{4.23}$$

But for the Sedov phase:

$$t_\mathrm{Sedov} = 3 \times 10^4\,\mathrm{yr}\, T_6^{-5/6} E_{51}^{1/3} n_\mathrm{H}^{-1/3} \tag{4.24}$$

Eq. (4.24) follows from solving Eq. (4.21) for t

Snow-plough Phase, II

Snowplough starts when $t_{\text{cool}} < t_{\text{Sedov}}$,

$$T_6 < E^{1/7} n_{\text{H}}^{2/7} \tag{4.25}$$

Expressing this in terms of the velocity:

$$v < 200\,\text{km}\,\text{s}^{-1}\,(E_{51} n_{\text{H}}^2)^{1/14} \tag{4.26}$$

almost independent from E and n.

Evolution during snowplough phase dominated by momentum conservation:

$$\frac{\text{d}p}{\text{d}t} = \frac{\text{d}}{\text{d}t}\left(\left(\frac{4\pi}{3}\right)\rho r^3 \dot{r}\right) = 0 \tag{4.27}$$

Remember: most mass is already in the shell!

Thus, if snowplough starts at radius r_0 and velocity v_0,

$$\frac{4\pi}{3}\rho r^3 \dot{r} = \frac{4\pi}{3}\rho r_0^3 v_0 \quad\Longleftrightarrow\quad r^3 \dot{r} = r_0^3 v_0 \tag{4.28}$$

Separation of variables gives

$$r(t) = r_0 \left(1 + \frac{4v_0}{r_0}(t - t_0)\right)^{1/4} \propto t^{1/4} \tag{4.29}$$

with $v_0 \sim 200\,\text{km}\,\text{s}^{-1}$,

$$v \sim 200\,\text{km}\,\text{s}^{-1}\left(\frac{t}{3\times 10^4\,\text{yr}}\right)^{-3/4} \tag{4.30}$$

Merging Phase

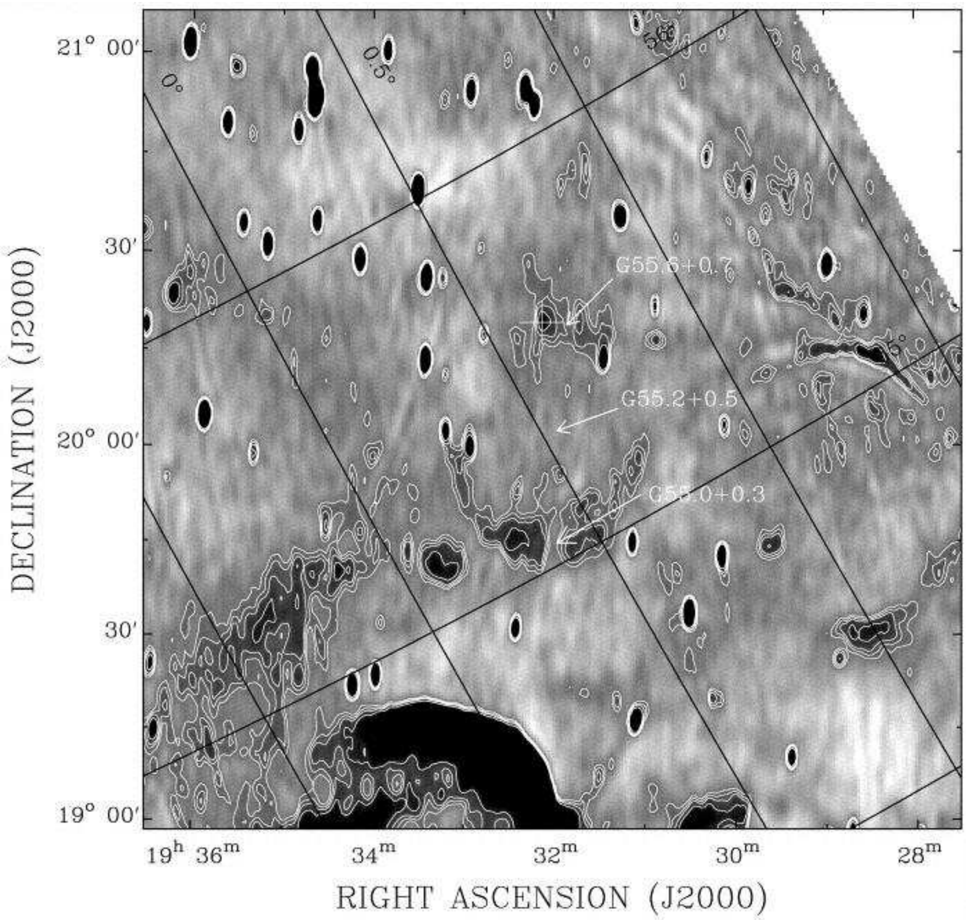

Radio map of G55.0+0.3 (1420 MHz, age $\sim 10^6$ years; Matthews et al., 1998)

Once speed drops to sound velocity of ISM,

$$c_{s,\mathrm{ISM}} \sim 10\ldots 100\,\mathrm{km\,s^{-1}} \tag{4.31}$$

supernova remnant starts to dissolve $\Longrightarrow$ Merging Phase

Elements produced during supernova mix into ISM ("chemical enrichment").

Summary

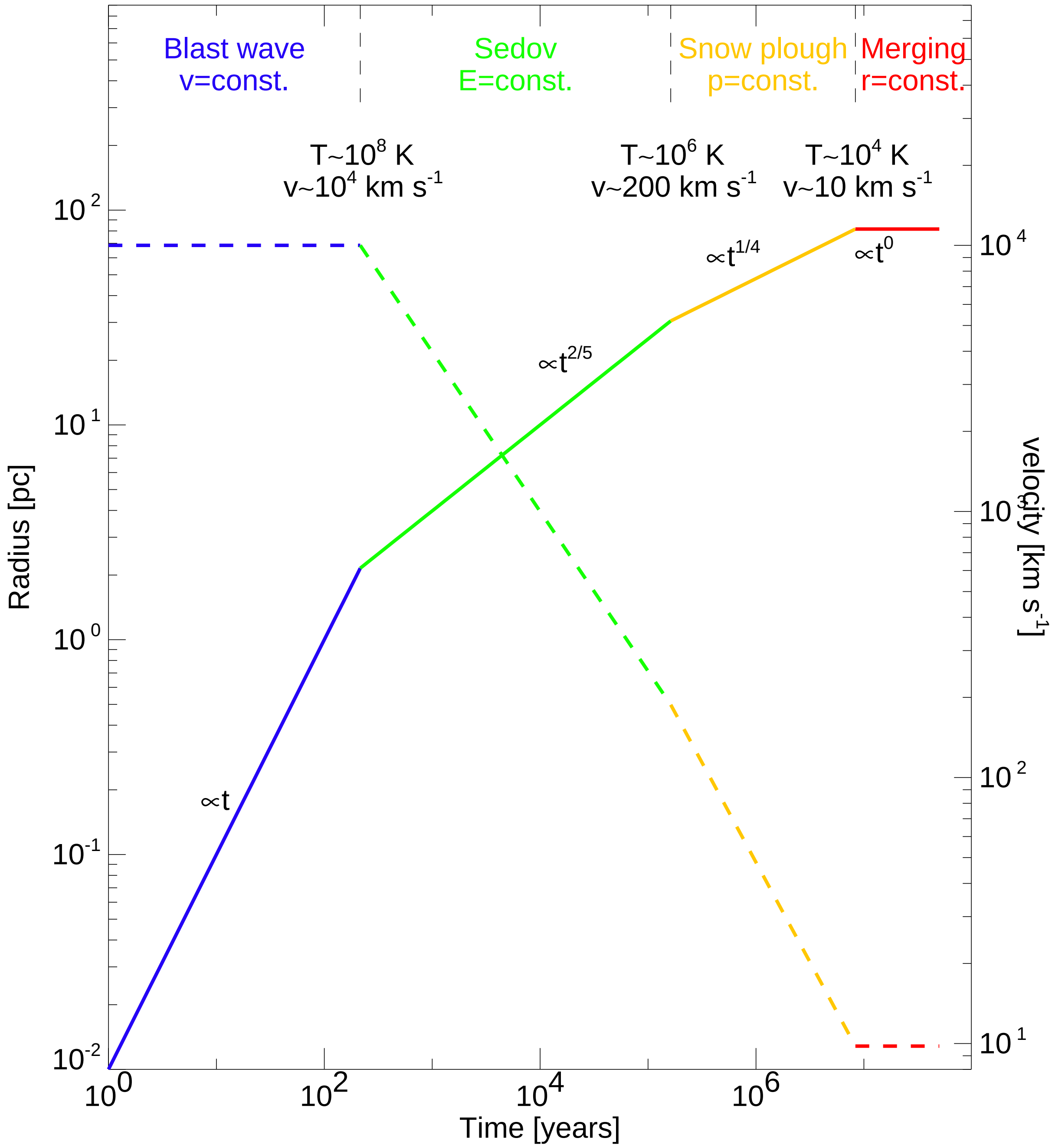

after Padmanabhan (2002, Fig. 4.6)

Bibliography

Anders, E., & Grevesse, N., 1989, Geochim. Cosmochim. Acta, 53, 197

Bałucińska-Church, M., & McCammon, D., 1992, ApJ, 400, 699

Brown, R. L., & Gould, R. J., 1970, Phys. Rev. D, 1, 2252

Burrows, D. N., et al., 2000, ApJ, 543, L149

Filippenko, A. V., 1997, ARA&A, 35, 309

Fireman, E. L., 1974, ApJ, 187, 57

Fitzpatrick, E. L., 1999, PASP, 111, 63

Fogel, M. E., & Leung, C. M., 1998, ApJ, 501, 175

Hasinger, G., Aschenbach, B., & Trümper, J., 1996, A&A, 312, L9

Mathis, J. S., 1996, ApJ, 472, 643

Mathis, J. S., Rumpl, W., & Nordsieck, K. H., 1977, ApJ, 217, 425

Mathis, J. S., & Whiffen, G., 1989, ApJ, 341, 808

Morrison, R., & McCammon, D., 1983, ApJ, 270, 119

Nicolosi, F., Jannitti, E., & Tondello, G., 1991, J. Physique IV, C1, 89

Ride, S. K., & Walker, Jr., A. B. C., 1977, A&A, 61, 339

Shull, J., 1993, Physica Scripta, T47, 165

Snow, T. P., & Witt, A. N., 1995, Sci, 270, 1455

Suntzeff, N. B., Phillips, M. M., Depoy, D. L., Elias, J. H., & Walker, A. R., 1991, AJ, 102, 1118

Yan, M., Sadeghpour, H. R., & Dalgarno, A., 1998, ApJ, 496, 1044